Multi-Phase Tectonic and Volcanic Evolution of a Nascent Backarc Rift: Impacts of Spreading Centre Reorientation, Subduction Reversals, Ridge Collisions, and Asymmetric Slab Rollback on the Northern New Hebrides Backarc

David J. Summer[a]*, Melissa O. Anderson[a], Philipp Brandl[b], Alan T. Baxter[c]

[a] Department of Earth Sciences, University of Toronto, 22 Ursula Franklin Street, Toronto, Ontario, M5S 3B1, Canada

[b] GEOMAR, Helmholtz Centre for Ocean Research Kiel, Wischhofstrasse 1-3, 24148 Kiel, Germany

[c] Department of Earth and Environmental Sciences, University of Ottawa, 75 Laurier Ave E, Ottawa, Ontario, K1N 6N5, Canada

Corresponding author: David Summer (david.summer@mail.utoronto.ca)

Key Points:

- Nascent backarc basin opening characterized by polyphase extensional periods prior to establishment of seafloor spreading
- Volcanic corridors exhibiting prolific volcanism occur along pre-existing crustal-scale structures and track arc migration

This is a non-peer reviewed preprint submission to EarthArXiv. This manuscript has been submitted to Tectonics for peer review.

Abstract

Intra-oceanic backarc are characterized by crustal accretion along seafloor spreading axes; however, little is known about the initial rifting of the over-riding plate prior to the establishment of stable seafloor spreading. To address this knowledge gap, we investigate the ~3.5 Ma backarc troughs in the New Hebrides Subduction Zone. Using available bathymetric data, we developed remote-predictive geologic maps at a scale of 1:100,000 over an area of ~234,000 km^2. Interpretation of seafloor morphologies, lineament analyses of seafloor fabric, fault kinematics revealed by earthquake moment tensor data, and cross-cutting relationships demonstrate distinct stress regime changes during sequential backarc rifting. South of 10.5°S, three phases of backarc opening are identified: 1) Initial arc rifting accommodating clockwise rotation of the arc, ~3.5–2.7 Ma (preserved in the Duff Horst and Graben Domain); 2) East-west-directed rifting and incipient seafloor spreading, ~2.7–1.1 Ma (preserved in the Jean Charcot Troughs); 3) Northeast-southwest- to NNE-SSW-directed rifting and counter-clockwise rotation of the arc, ~1.1 Ma-present (preserved in the actively rifting Santa Cruz Troughs). Two prominent roughly east-west oriented backarc volcanic corridors stretch from the relict arc and track arc migration along deep crustal-scale structures. North of ~10.5°S, two grabens formed from a single rift event occurring before the crustal scale ruptures that severed the Reef Islands Platform from the New Hebrides Arc. The outcome of this work reveals new insights in the geodynamic processes that bridge periods of stable subduction with the formation of mature backarc basins with crustal accretion occurring along spreading axes.

Plain Language Summary

In oceanic subduction zones, extensional backarc basins form from seafloor spreading, however, little is known about the early phases of basin formation before seafloor spreading is established. To address this knowledge gap, we investigate the ~3.5 Ma backarc basin in the New Hebrides Subduction Zone. Using available bathymetry data, we developed geological maps at a scale of 1:100,000 over an area of ~234,000 km^2. Geological interpretations of these maps as well as current patterns of faulting revealed by earthquake data reveal episodic basin opening. South of ~10.5°S, three phases are identified: 1) Initial arc rifting during clockwise rotation of the arc, ~3.5–2.7 Ma; 2) East-west-directed rifting leading up to initiation of seafloor spreading, ~2.7–1.1 Ma; 3) Northeast-southwest-directed rifting during a phase of counterclockwise arc rotation; ~1.1 Ma–present. Two zones of prominent volcanism are observed in the backarc and trail behind the migrating arc. North of ~10.5°S, a single rift event occurred, becoming inactive following the formation of a major fault at that latitude, which isolated this region from the active subduction zone to the south. The outcomes of this study reveal new insights into the processes of backarc rifting between stable subduction and the establishment of spreading centres.

1 Introduction

Intra-oceanic backarc basins form at convergent boundaries where the sinking of dense oceanic lithosphere induces hinge retreat/slab rollback and/or migration of the overriding plate away from the trench promotes rifting in the overriding plate (Sleep and Toksöz, 1971; Uyeda and Kanamori, 1979; Taylor and Karner, 1983; Sdrolias and Müller, 2006). The conceptual model for backarc basin opening on the overriding plate in response to extension involves the initiation of rifting in the weakest region of the overriding plate (e.g., the volcanic arc; Karig, 1970; Molnar and Atwater, 1978), crustal thinning with progressive rifting, and basin maturation achieved via the establishment of seafloor spreading (Martinez et al., 1995; Taylor et al., 1996; Caratori Tontini et al., 2019). Coeval with these tectonic phases, hydrous, low-viscosity arc magmatism is displaced trenchward by anhydrous, MORB-like mantle upwelling as seafloor spreading is established (Dunn and Martinez, 2011). In addition to the presence of seafloor spreading, mature backarc basins are characterized by sudden changes in the position or orientation of spreading centres, greater surface depths relative to oceanic basins with equivalent ages, and a longevity on the order of tens of millions of years (Tamaki and Honza, 1991), after which the basin closes via subduction. Unlike mature backarc basins, the early rifting phases of backarc basin opening are short-lived, quickly yielding to seafloor spreading (Dunn and Martinez, 2011; Caratori Tontino et al., 2019). Indeed, most modern backarc basins feature seafloor spreading and little is known about the geodynamics during rift initiation and early crustal rifting in backarc basins.

The New Hebrides Subduction Zone (NHSZ) (**Fig. 1**) is a NNW-SSE-oriented oceanic convergence zone where relict backarc basins on the Australia Plate subduct beneath the New Hebrides Arc (NHA) along a length of ~1500 km. On the overriding plate within the northern end of this subduction zone, a nascent backarc basin exhibits tenuous evidence for the presence of axial spreading, suggesting that the backarc is likely in the early rifting stages of basin opening. Luyendyk et al. (1974) suggest that high heat flow,

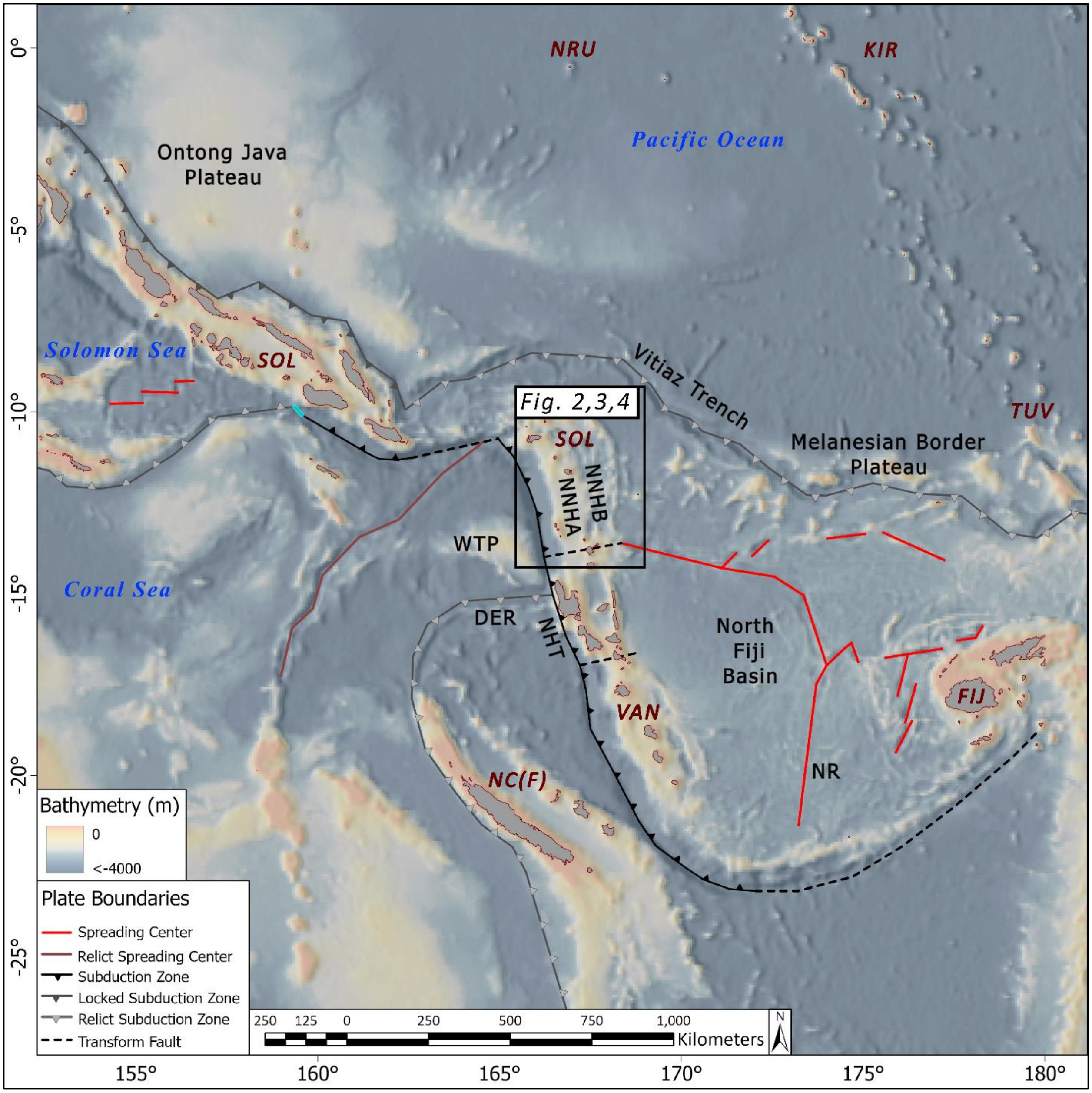

Figure 1. Regional bathymetric map of the Southwest Pacific featuring active and relict tectonic boundaries. Notable tectonic features: DER = D'Entrecasteaux Ridge, NFB = North Fiji Basin, NNHA = North New Hebrides Arc, NNHB = North New Hebrides Backarc, NHT = New Hebrides Trench, NR = Nova Rise, WTP = West Torres Plateau. Nation states: KIR = Kiribati, NC(F) = New Caledonia (France), NRU = Nauru, SOL = Solomon Islands, TUV = Tuvalu, VAN = Vanuatu.

negative gravity anomalies, and positive magnetic anomalies, serve as indicators for early seafloor spreading within the extensional troughs of the northern NHB. This was later supported by the presence of backarc basin basalts in the backarc troughs (Monjaret et al., 1990). Since then, bathymetric, magnetic and seismic studies have concluded that the northern NHB is a zone of crustal extension, absent seafloor spreading (e.g., Charvis & Pelletier, 1989). Monjaret et al. (1990) suggest that opening of the troughs was a polyphase event, as indicated by pulses of magmatism throughout the basin's history. Paleomagnetic studies reveal a history of clockwise rotation of the New Hebrides Arc (NHA; Falvey, 1978; Musgrave & Firth, 1999), while geodetic studies show that the northern NHA is currently rotating counterclockwise (Calmant et al., 2003; Bergeot et al., 2009). This contrast in microplate geodynamics supports the hypothesis of polyphase sequence of basin opening in response to sequential regional tectonic events. The impacts of these tectonic events on the spatio-temporal evolution of basin opening and associated patterns of volcanism in the northern NHB have not been fully resolved. To this end, we investigate the evolution of the northern NHB troughs by compiling available bathymetric and seismic data in GIS software and interrogating the morphological and structural character of the basin. Furthermore, we infer correlations between phases of basin opening and previously described regional tectonic events. These events include: the clockwise rotation of the arc prior to ~3 Ma, the formation of a Subduction Transform Edge Propagator (STEP) fault, spreading axes rearrangement in the North Fiji Basin (NFB) since ~10 Ma, arc collisions with buoyant oceanic features, and changing dynamics of the subducting slab.

2 Tectonic history

During the Eocene, the NHA was part of the Melanesian Arc, which included present-day arc segments stretching from the New Britain Arc to the Tonga-Kermadec Arc, accommodating SW-vergent subduction of the Pacific Plate beneath the Australia Plate along the Vitiaz Trench (**Fig. 1**; Crooks and Belbin; 1978; Hall, 2002; Schellart et al., 2006). Arrival of the Ontong Java Plateau and the Melanesian Border Plateau during the Miocene resulted in locking of the Solomon and New Hebrides segments of the Melanesian Arc by ~18 Ma (Pelletier et al., 1993; Schellart et al., 2006). By ~10 Ma, the plateau collisions induced a subduction polarity reversal, initiating subduction of the Indo-Australia Plate to the NE along the New Hebrides Trench (NHT) and the South Solomon Trench (Falvey, 1975; Musgrave & Firth, 1999; Petterson et al., 1999). Following subduction initiation, asymmetric rollback of the Australia Plate induced a “double saloon-door” style of opening of the North Fiji Basin (NFB) and clockwise rotation of the NHA by 30–52° to its present-day position (Falvey, 1978; Auzende et al., 1988; Musgrave & Firth, 1999; Martin, 2013). The rotation of the NHA resulted in a sharp, nearly 90° bend in the trench at the northern termination between the South Solomon Trench and the NHT (10.8°S, 164.8°E), producing a tear in the subducting slab and forming the San Cristobal Fault, a subduction-transform edge propagator fault, at this intersection (Neely & Furlong, 2018).

At ~2–3 Ma the D’Entrecasteaux Ridge, a relict Eocene arc, arrived at the central portion of the NHT (15–16°S; Macfarlene et al., 1988; Greene et al., 1994). This resulted in segmentation of the subduction zone, with a central compression belt in the central segment separating extensional zones to the north and south (Greene et al., 1994; Pelletier et al., 1998; Calmant et al., 2003; Anderson et al., 2016). Coeval with this collision, a change in regional stress fields resulted in the abandonment of N-S-directed spreading in the NFB and the establishment of an E-W-directed spreading centre, the Nova Rise, at ~174°E between ~16–21°N (Auzende, 1990). This was followed by the arrival of the West Torres Massif, a buoyant submarine feature of unknown origin, to the north of the D’Entrecasteaux Ridge, at ~1.0–0.7 Ma, further slowing convergence in the central portion of the subduction zone (Meffre and Crawford, 2001).

Currently, the subduction zone convergence rate is ~40 mm/yr at ~13.5°S and increases northward to a maximum of 150–170 mm/yr at ~10°S. In the northern end of the subduction zone, convergence is accommodated by backarc extension at a rate of up to ~60–80 mm/yr, associated with an overall counterclockwise rotation of the northern segment of the arc (Pelletier et al., 1998; Calmant et al., 2003; Bergeot et al., 2009). The northern NHB is ~60 km across at ~13.5°S and widens northward to ~130 km across at ~10°S, where the backarc troughs reach a maximum depth of ~4000 m and terminate abruptly at a ~2 km high escarpment.

3. Data and methods

Remote-predictive geologic mapping of the northern New Hebrides subduction zone is achieved through the interpretation of remotely acquired ship-track multibeam echosounder bathymetry data. In this process, bathymetry raster datasets are used to visualize the seafloor in GIS software (ArcGIS). Classifications schemes for the remote-predictive geologic and the structural maps of the study area are developed with reference to seafloor morphology and tectonic setting, following previous mapping approaches (c.f. Anderson et al., 2016; Klischies et al., 2019, Baxter et al., 2020, Stewart et al., 2022). Maps are produced at a scale of 1:100 000 over an area of ~234 000 km^2. Centroid moment tensor (CMT) data, where available, are used to resolve fault kinematics in seismically active zones. The culminated geologic and structural maps, fault kinematics, and lineament analyses are used to interpret the stress regime changes and associated spatio-temporal backarc rift domains.

3.1 Bathymetric data

Bathymetric data included in this study are sourced from the following cruises: SOPACMAPS LEG 1 (Daniel, 1993), LEG 2 (Auzende, 1993), and LEG 3 (Pelletier, 1993), MGL0904 (Johnson, 2009), and DUKE15 (Crowhurst, 2015). Visualization of high-quality data is achieved in ArcGIS software, and the bathymetric data, ranging from 25–150 m resolution, are layered in descending order of resolution. Areas lacking ship-track bathymetry coverage are underlain by the General Bathymetric Charts of the Oceans terrain model (GEBCO Compilation Group, 2023). Multi-directional hillshade and slope raster datasets underlay each bathymetry raster layer with variable transparencies for each to achieve a three-dimensional effect for data visualisation.

3.2.1 Tectonic settings and remote-predictive geologic mapping

Geologic classification of the northern New Hebrides subduction zone was embedded in five tectonic settings: forearc, arc, arc-backarc transition, backarc, and relict arc. The criteria for tectonic settings are as follows: (1) The New Hebrides Forearc is the terrain that slopes from the arc platform towards the NHT; (2) the New Hebrides Arc (NHA) is the relatively shallow, sedimented, flat-lying platform (<2000 m depth) 60–80 km inboard from the trench; (3) The New Hebrides arc-backarc transition is variably faulted terrain that slopes eastward from the arc towards the deeper backarc; (4) The New Hebrides Backarc (NHB) is the terrain characterized by numerous extensional troughs and variable deformational and volcanic morphologies lying between the arc-backarc transition and the relict arc; (5) The relict arc is characterised by either a ridgeline or horst and graben morphology separating the NHB from the North Fiji Basin (NFB). This domain also includes the Reef Islands Platform (RIP), a northern continuation of the NHA that has been severed from the westward migrating active arc to the south. In addition, features in the neighbouring NFB to the east and the subducting Santa Cruz Basin to the west are separate tectonic domains that constitute a sixth classification but are not described in detail here. The classification of geologic features embedded within the tectonic groupings is presented in Table 1.

Table 1

Classification criteria for remote-predictive geologic mapping units

Bathymetry	Mapped feature	Feature morphology	Variations
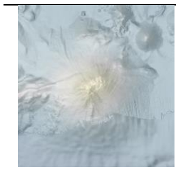	Volcano	Conical, radially sloped edifice, concave at it’s base, with pointed or cratered peak, >2 km in width	Classification dependent on tectonic location; arc, backarc, or relict arc
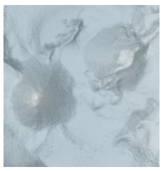	Small volcano	Conical, radially sloped edifice, concave at it’s base, <2 km in width, often occurring in clusters in close proximity to larger central volcanoes	Classification dependent on tectonic location; arc, backarc, or relict arc
	Rifted volcano	Conical, radially sloped edifice, concave at it’s base, with pointed or cratered peak, heavily faulted; rifted halves often occur on opposing sides of a trough, with rifting occurring along a peripheral dyke	Classification dependent on tectonic location; arc, backarc, or relict arc
	Volcanic fissure	Linear structures with symmetrically sloped sides; often occur in clusters in close proximity to a large central volcano and are associated with terrain featuring hummocky lava flows	Classification dependent on tectonic location; arc, backarc, or relict arc
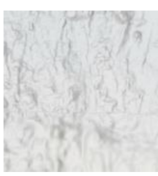	Hummocky terrain	Areas of high surface irregularity revealed by small mounds and depressions; often associated with expansive lava flows in volcanically active regions	Variations include the arc and relict arc setting, shallow volcanic corridors, deeper slopes of volcanic corridors, and volcanically active troughs
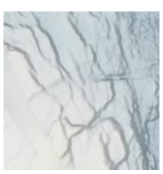	Faulted terrain	Areas of abundant faulting; faults present as linear features with an abrupt change in relief on either side of the lineament	Variations include the backarc setting and the arc-backarc transitional slope
	Trough	Elongated, often discontinuous depressions, bound by footwall scarps or hummocky sloped terrain; trough floors may be sedimented or hummocky	Troughs occur in backarc and relict arc settings
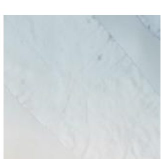	Sedimented terrain	Areas of smooth, flat-lying or gently sloped terrain	Variations include the arc and relict arc platforms, and relict arc and backarc troughs

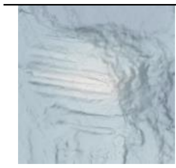	Oceanic core complex	A domal structure with surficial corrugations; linear features with very subtle changes in relief	N/A
	Uplifted forearc	Area of forearc crust significantly shallower (>1500 m) than trench-parallel forearc segments with subaerial exposure and faulted slopes	N/A
	Ridgeline/ horst	Peaked ridgelines, continuous or discontinuous and anastomosing, often with asymmetrical slopes on either side of tilted horsts	Continuous ridgelines characteristic of the northern relict arc; discontinuous, anastomosing horsts characteristic of southern relict arc
	Debris flow	Lobed and smooth structure, gently sloping away from shallower terrains; steeply sloped toe	N/A
	Spreading axes	Deep axial valley with faulted morphology on opposing sides with valley ridge crest rising to the basin floor	N/A
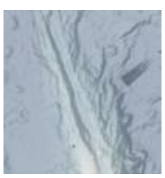	Leaky transform fault	Singular or multiple subparallel fault lines stretching several tens of kilometers; associated with volcanoes, volcanic fissures and hummocky terrain	N/A
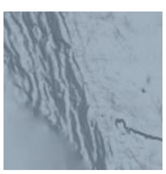	Trench	Continuous, >6 km deep, linear depression, seismically active, demarcating the subduction zone boundary; the down going plate has a heavily faulted morphology whereas the opposing forearc has a smooth, sedimented morphology	N/A

3.3.2 Structural mapping, lineament analysis, and fault kinematics

Mapped structures include volcanic fissures, normal faults, thrust faults, corrugations, and detachment faults. Volcanic fissures are identified as linear peaks in the bathymetry with symmetrical slopes on either side. Normal faults are identified as asymmetrical linear features with a steep slope separating areas of contrasting relief. The morphology of thrust faults resembles that of normal faults, however, they are interpreted to occur in the forearc where crustal uplift must be accompanied by compressional tectonics. Corrugations lack an appreciable change in relief and are located on a single domal structure interpreted to be an oceanic core complex. The contact between the core complex and the surrounding seafloor is therefore interpreted to be a low-angle detachment fault.

Lineaments are classified into eight 22.5° intervals and lineament orientation maps are produced to reveal patterns of lineament trends across the mapping area (**Fig. 4**). The range of lineament lengths varied from ~100 m to several tens of kilometres. All lineaments were broken up into 100 m segments to ensure that each lineament feature was proportionally represented during analyses. The 100 m segmented lineament data is represented in rose diagrams to show the distribution of lineament orientations across spatio-temporal backarc domains.

Where possible, the fault kinematics were resolved by interpreting centroid moment tensor data together with local lineament features following the approach of Baxter et al. (2020). The CMT data for earthquakes with M_w >5.0 and depths of <30 km (n = 53) were acquired from the global CMT project (Dziewonski et al., 1981; Ekström et al., 2012). The dataset was imported into the ArcGIS project using the Arcbeachball tool. Each CMT has two possible focal plane solutions for the earthquake; the interpretation of the likely fault plane is based on comparisons with the dominant lineament trends at surface, following Baxter et al. (2020). Where the focal plane of a CMT could not be resolved (e.g., due to the absences of high-resolution ship-track bathymetry), CMTs were classified as “unresolved fault types.” Taken together, mapped morphotectonic and structural features, lineament orientations, and fault kinematics were used to interpret the history of stress regime changes during progressive backarc opening.

4 Geology and structure of the northern New Hebrides Backarc

The geologic, structural, and lineament orientation maps of the New Hebrides Subduction Zone (NHSZ) achieved using a remote-predictive mapping approach are presented in **Figures 2, 3,** and **4**, respectively. A total of 36 distinct morphotectonic units were mapped and a total of 16,000 lineaments occur throughout the mapping area including ~14,000 normal faults with throws ranging from ~20–2,000 m, and just under 2,400 volcanic fissures rising up to ~500 m from the surrounding seafloor. Lineaments vary from ~100 m to several tens of kilometres and lineament orientations are variable throughout the study area. Below, we describe in detail the tectonic domains that are relevant to the spatio-temporal geodynamic history of the subduction zone. Where there are significant differences in the geologic or structural expression within a given setting, we subdivide the descriptions accordingly. Specifically, we provide descriptions for the northern and eastern relict arc rifts, the central and northwestern backarc rifts, as well as the arc-backarc transition together with the arc platform.

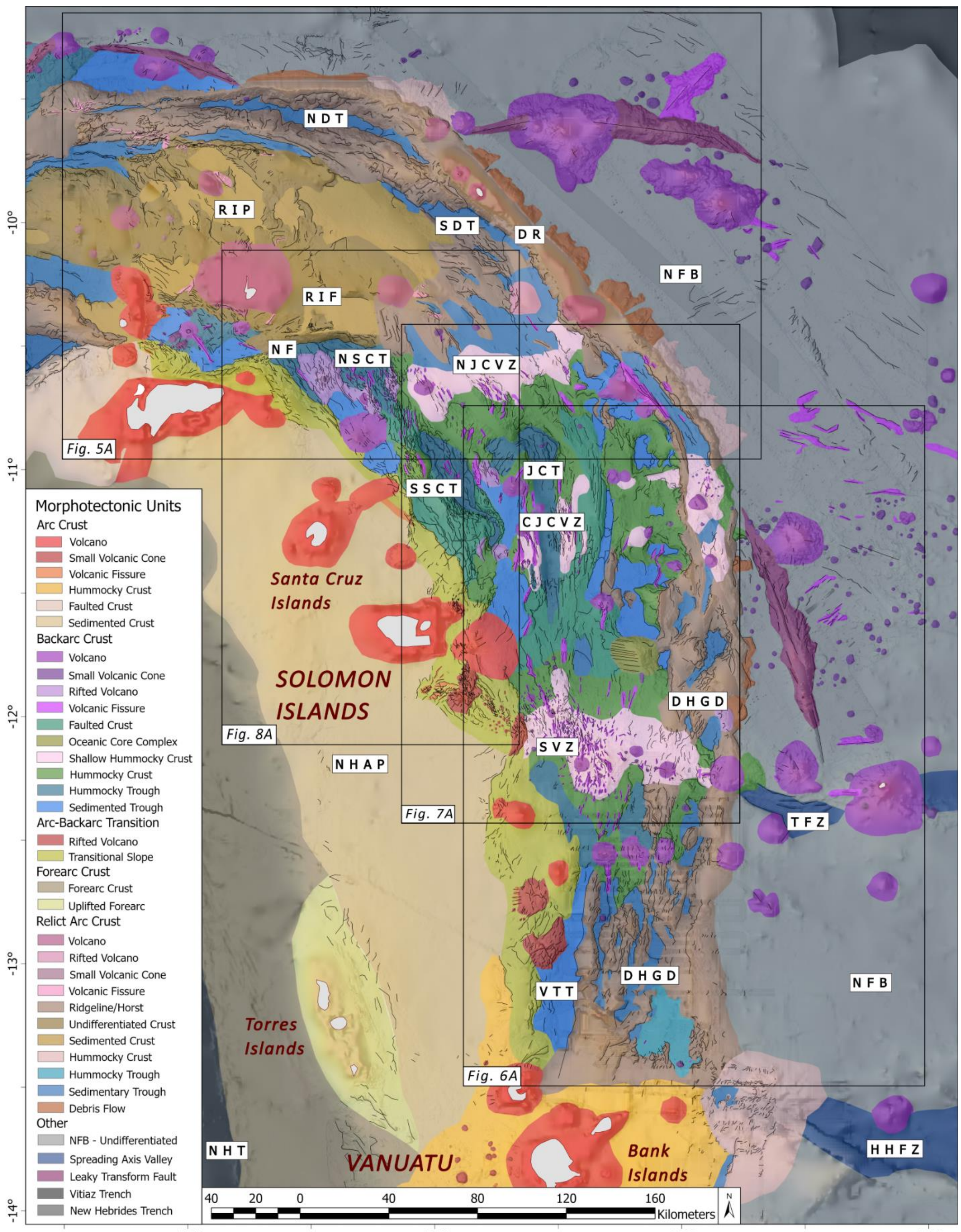

Figure 2:Morphotectonic map of the North New Hebrides Subduction Zone. Criteria for classification are presented in Table 1. CJCVZ = Central Jean Charcot Volcanic Zone, DHGD = Duff Horst and Graben Domain, DR = Duff Ridge, HHFZ = Hazel Holme Fracture Zone, JCT = Jean Charcot Trough,

NF = Nendö Fault, NDT = North Duff Trough NFB = North Fiji Basin, NHT = New Hebrides Trench, NHAP = New Hebrides Arc Platform, NJCVZ = North Jean Charcot Volcanic Zone, NSCT = North Santa Cruz Trough RIF = Reef Islands Fault, RIP = Reef Islands Platform, SDT – South Duff Trough, SSCT = South Santa Cruz Trough, SVZ = Starfish Volcanic Zone, TFZ = Tikopia Fracture Zone, VTT = Vot Tande Trough.

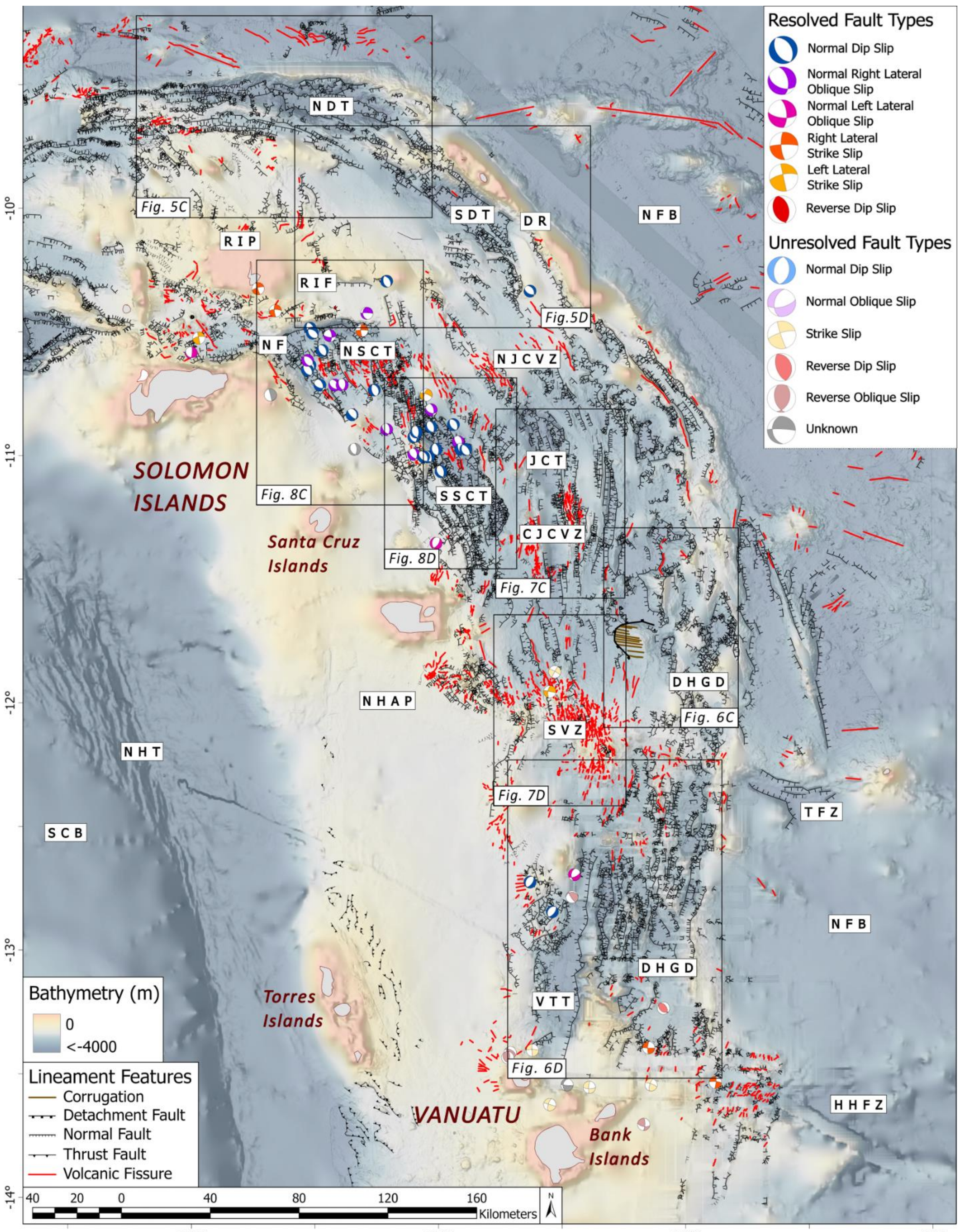

Figure 3: Structural map of the North New Hebrides Subduction Zone. SCB = Santa Cruz Basin; all other acronym meanings provided in Figure 2 caption.

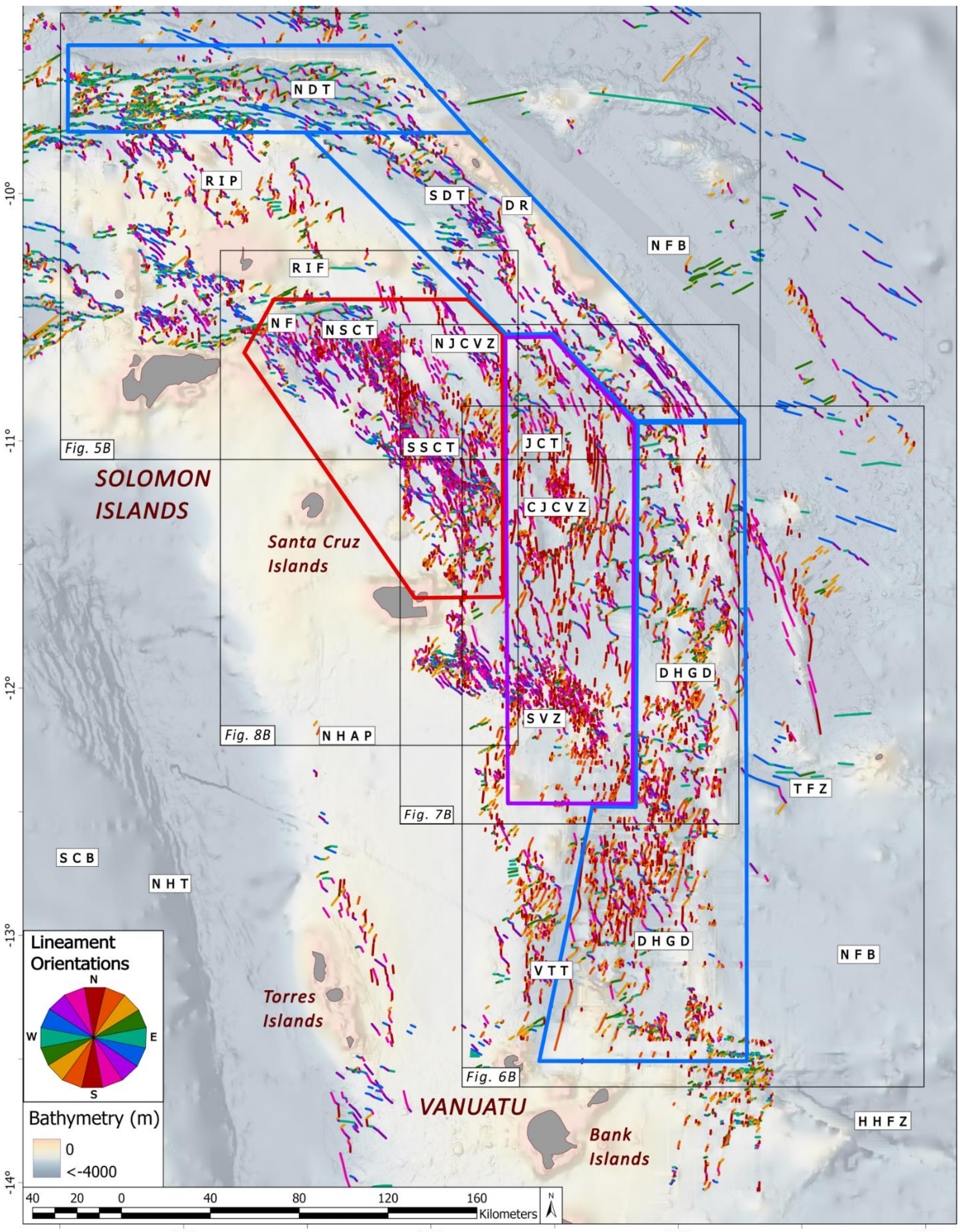

Figure 4: Lineament orientation map of the North New Hebrides Subduction Zone. Coloured polygons are approximate boundaries of spatio- temporal stages of backarc opening: blue = Relict Arc Rifts, purple = Jean Charcot Rift, red = Santa Cruz Rift. Acronym meanings provided in Figure 2 and 3 captions.

4.1 Relict arc rifts

The northern NHSZ is characterized by two relict arc features, the Reef Islands Platform (RIP) and the Duff Ridge (DR), which, have been rifted along two sedimented troughs. The DR is a single ridgeline that forms the boundary between the NHSZ and the NFB to the east. The active arc platform is offset to the west of the RIP by at least 55 km along an E-W-trending escarpment; sharply contrasting morphologies and lineament orientations to the south indicate that the escarpment forms a microplate boundary between the RIP and regions to the south which, are therefore described as separate spatio-temporal domains. Regarding the relict arc, a region of horsts and grabens, referred to here as the Duff Horst and Graben Domain (DHGD), extend south from the DR and form a zone of diffuse, rifted relict arc crust.

4.1.1 The relict arc rifts: The Duff Ridge and The Reef Islands Platform

The DR has an arcuate shape subparallel to the trench and is most prominent along a NW-SE trend between 166.7°E, 9.5°S and 167.8°E, 10.5°S (**Fig. 5a**). A subaerial exposure of the ridge occurs at 167.1°E, 9.8°S (the Duff Islands). The ridgeline records the position of the northern-most NHA prior to rift initiation (e.g., Auzende et al., 1995). The RIP is a shallow (>2,000 mbsl), sedimented, and largely undeformed region with numerous volcanic edifices. The region separating the RIP from the DR features two sedimented grabens (flat, smooth morphology) referred to here as the Duff Troughs (DT), which are elongated parallel to the ridgeline and separate it from the RIP to the south and to the west. The northern-most graben is elongated E-W and has lineament orientation peaks trending 85–90° and 110–115° (**Fig. 5b**). Referred to here as the north DT, it reaches depths of ~4,300 m and is bound to the south by a series of fault scarps with a cumulative throw of ~3,000 m rising southward to the RIP (**Fig. 5c**). South of the this, a smaller, shallower trough is nested within the series of fault scarps. Southeast of the north DT, a second trough referred to here as the south DT has peak lineament orientations of 140–145° (**Fig. 5b**).

This trough reaches depths of ~3600 mbsl and is bound by a ~500 m footwall scarp to the SW, from which the RIP shoals towards the Reef Islands to the west (**Fig. 5d**). South of this graben is a zone of deformation featuring E-W to N-S trending fault scarps forming a series of arcuate geometries that step southwestward and eventually terminate at two crustal-scale, E-W trending faults, referred to here as the Reef Islands Fault and the Nendö Fault, the latter forming the microplate boundary between the RIP and the backarc. At the southeast end of the DR, the ridgeline is rifted by a single ~10 km wide basin which curves to a N-S trend beyond which the Duff Ridge yields to a discontinuous arrangement of horst and graben structures, the DHGD.

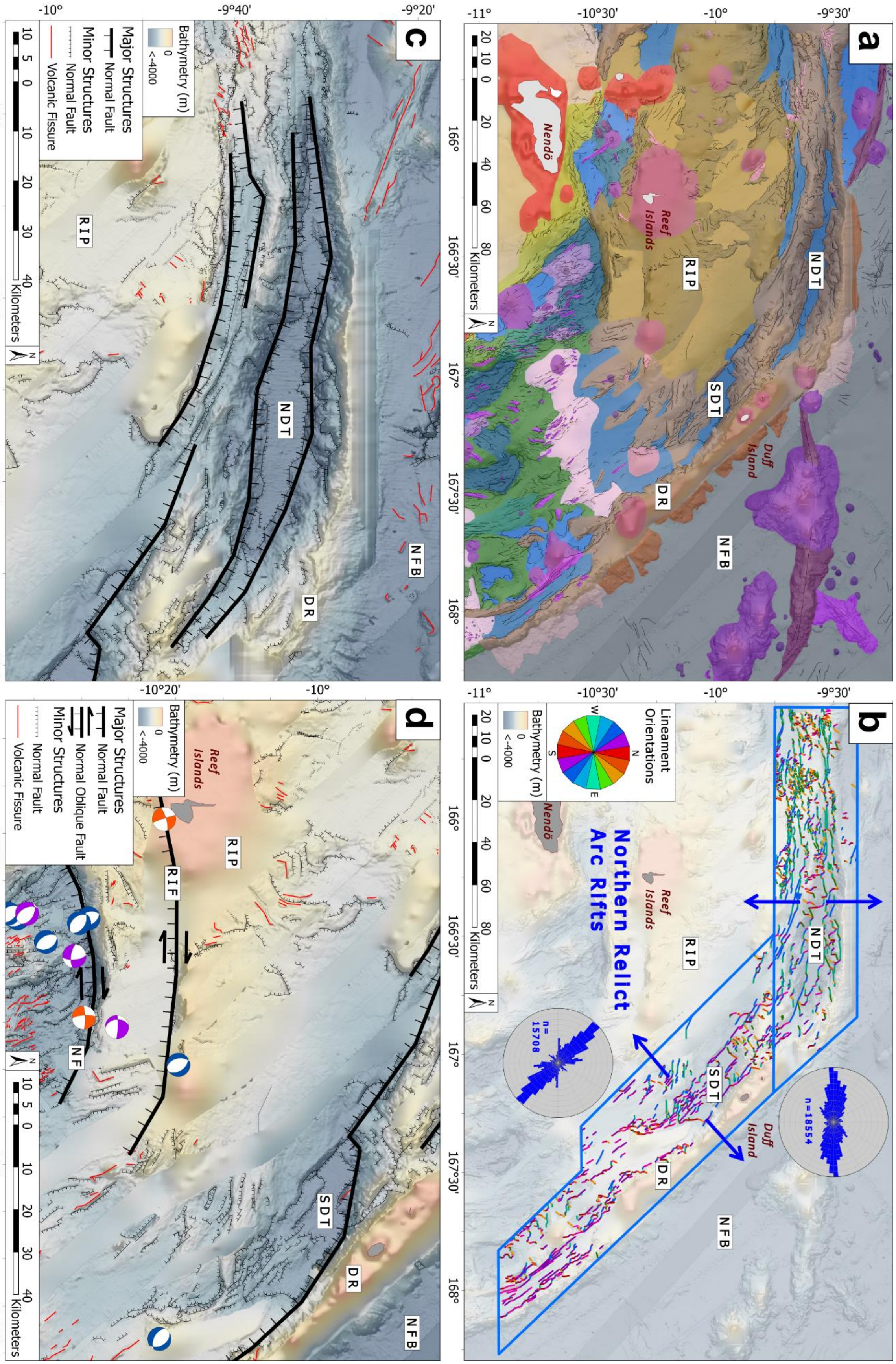
a
b
c
d
NDT
SDT
DR
NFB
RIP
RIF
NF
Nendö
Reef Islands
Duff Island
Northern Rellict Arc Rifts
Lineament Orientations
n=18554
n=15708
Bathymetry (m)
0
<-4000
Major Structures
Normal Fault
Normal Oblique Fault
Minor Structures
Normal Fault
Volcanic Fissure
Kilometers
-9°20'
-9°30'
-9°40'
-10°
-10°20'
-10°30'
-11°
166°
166°20'
166°30'
166°40'
167°
167°20'
167°30'
168°

Figure 5: A) Morphotectonic map of the Northern Relict Arc Rift; B) Lineament orientation map of the North Duff Trough and South Duff Trough. Blue arrows indicate the opening of these two troughs and the rifting of the Reef Islands Platform from the Duff Ridge and the North Fiji Basin; C) Structural map of the North Duff Trough. Steep escarpments bound the trough with the Duff Ridge to the north and the Reef Islands Platform to the south. A second narrow and shallow basin is structurally adjoined to the North Duff Trough; D) Structural Map of the South Duff Trough. To the northwest, a steep escarpment rises to the Duff Ridge, contrasting with the gently sloped rise to the Reef Islands Platform, indicating a detatchment fault underlies the to the South Duff Trough and the Reef Islands Platform. A pattern of arcuate faulting is found between the South Duff Trough and the Nendö Fault. Acronym meanings provided in Figure 2 caption.

4.1.2 The New Hebrides relict arc rift: Duff Horst and Graben Domain

The DHGD extends from ~11°S to ~13.5°S, widening from ~20 km in the north to ~60 km in the south, terminating at the New Hebrides compression zone (**Fig. 6a**). Lineament orientation peaks are 0–5° and 20–25° throughout this region of the relict arc (**Fig. 6b**). The relict arc is characterized by an arrangement of tilted horst structures with prominent, anastomosing W- to WNW-dipping fault scarps which bound discontinuous sedimented half-grabens (**Fig. 6c**). Further south at ~12.2°S, the relict arc intersects the Tikopia Fracture Zone, a relict NFB spreading centre. At this intersection, a series of backarc volcanoes surrounded by shallow hummocky terrain and numerous volcanic fissures and small cones interrupt the otherwise continuous N-S arrangement of horst structures. This volcanic terrain forms an E-W oriented volcanic belt called the Starfish Volcanic Zone (SVZ) that extends westward to the active arc. South of this intersection, the relict arc is more heavily faulted and consists of smaller horst structures, and lower relief footwall scarps lacking a prevalent dip-direction (**Fig. 6d**). The exception to this is a single, prominent ~100 km long escarpment, which is a boundary fault separating the relict arc DHGD from a single narrow backarc trough, the Vot Tande Trough (VTT). To the southeast of the DHGD, the New Hebrides Subduction Zone intersects the Hazel Holme Fracture Zone, which is an ultra-slow E-W trending spreading centre in the NFB. This intersection also separates the extensional north NHSZ from the compressional zone the south and features numerous CMTs revealing strike-slip to reverse oblique slip fault kinematics.

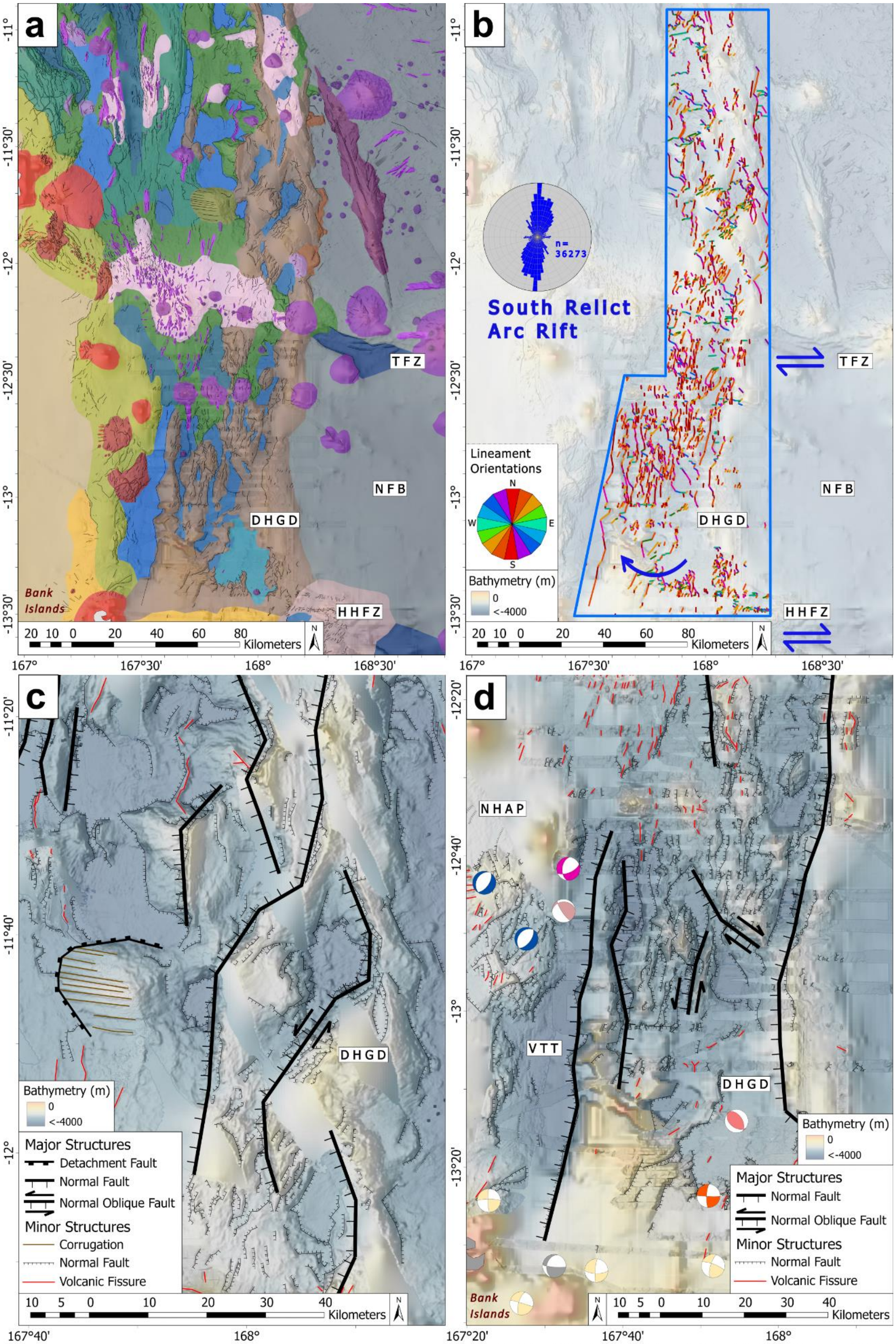
a
b
c
d
South Relict
Arc Rift
n=
36273
TFZ
NFB
DHGD
HHFZ
Bank
Islands
NHAP
VTT
Lineament
Orientations
Bathymetry (m)
0
<-4000
Major Structures
Detachment Fault
Normal Fault
Normal Oblique Fault
Minor Structures
Corrugation
Normal Fault
Volcanic Fissure
Kilometers
-11°
-11°30'
-12°
-12°30'
-13°
-13°30'
167°
167°30'
168°
168°30'
-11°20'
-11°40'
167°40'
-12°20'
-12°40'
-13°20'
167°20'

316

Figure 6: A) Morphotectonic map of the Southern Relict Arc Rift—the Duff Horst and Graben Domain; B) Lineament orientation map of the Duff Horst and Graben Domain. Blue double arrows indicate the interpreted dextral strikeslip component of fault kinematics along the Hazel Holme Fracture Zone and the Tikopia Fracture Zone during arc rifting. Curved arrow indicates clockwise rotation of the New Hebrides Arc Platform resulting from arc riftin; C) Structural map of a section of the Duff Horst and Graben Domain north of the Tikopia Fracture Zone showing the anastomosing arrangement of horst structures with west dipping fault scarps. Rifted crators reveal the volcanic edifices were the focus of rifting. D) Structural map of the Duff Horst and Graben south of the Tikopia Fracture Zone showing a region of heavily fragmented horst structures and conjugate faulting accomodating transtensional breakup of the arc. A ~100 km long fault scarp east of the Vot Tande Trough and a gently sloped arc/backarc transition zone to the west indicates a detachment fault underlies the Vot Tande Trough and the arc/backarc transition zone. Acronym meanings provided in Figure 2 caption.

4.2 The backarc rifts

The NHB troughs are bordered by the arc-backarc transition to the west, the RIP to the north, the DHGD to the east and the New Hebrides compressional zone (the Bank Islands) to the south. The NHB is characterised by variably hummocky or faulted crust throughout. Generally, troughs and lesser depressions are sedimented to the east and hummocky morphologies prevail to the west and northwest. Prevailing lineament orientations are N-S-trending to the west of the DHGD, and NNW-SSE to NW-SE-trending further to the northwest. In this study, we distinguish the Jean Charcot Troughs (JCT) from the Santa Cruz Troughs (SCT) based on whether prevailing lineament trends are N-S or NNW-SSE to NW-SE, respectively.

4.2.1 The central backarc rift: The Jean Charcot Troughs and the Vot Tande Trough

The Jean Charcot Troughs (JCT) in the central portion of the backarc are characterized by variable seafloor morphologies including areas exhibiting abundant volcanism, a flat, sedimented morphology, or high densities of faulting (**Fig. 7a**). Across this domain, lineament orientations are remarkably uniform with only slight deviations from the 175–185° orientation peak (**Fig. 7b**). In the north, the JCT is bound by an ENE-WSW-oriented volcanic corridor along 10.6°S, where NNW-SSE-trending volcanic fissures deviate from the N-S lineament trends in the JCT. The hummocky terrain of the 10.6°S volcanic zone gradually deepens southward from ~1,700 mbsl to a maximum depth of ~3,900 mbsl at the northern extent of the JCT. Here, a singular prominent trough, the central JCT is a hummocky-bottomed trough, is elongated N-S, and narrows southward, becoming a ~10 km wide valley within a second zone of focused magmatism centred at 11.3°S. The relatively gentle hummocky slopes enveloping the north end of the central JCT transition into steep fault scarps within the 11.3°S volcanic zone that reach throws of up to ~1,700 m and lengths of up to ~80 km (**Fig. 7c**). The 11.3°S volcanic zone rises to depths above 2,300 mbsl on either side of the ~3,400–3,200 mbsl deep axial valley floor and features large volcanic cones and abundant volcanic fissures covering an area of ~1,500 km^2. Despite the absence of seismic activity, the axial valley floor has a hummocky morphology indicating recent volcanic activity. To the east of this valley and parallel to it is a long, narrow valley that has a flat-bottomed morphology, indicating abundant sedimentation. To the south of the 11.3°S volcanic zone, the central JCT opens into a zone ranging from ~3,400–2,600 mbsl in depth, bound to the west by the arc-backarc transition and to the east by a previously undescribed oceanic core complex (OCC) centred at ~167.8°E, 11.8°S. This OCC has a domal morphology, rising to a depth of 1,900 m. Corrugations on the exhumed surface record an extension direction consistent with the principal WNW-ESE extension recorded in the DHGD. This region is characterized by a sparsity of volcanic features and abundant low relief normal faults that bound numerous small, indistinct troughs/depressions with variable hummocky to sedimented morphologies. Further to the south, the seafloor shoals up to the SVZ (**Fig. 7d**), located between ~12.0–12.5°S and covering an area slightly larger than the 11.3°S volcanic zone. Like the 11.3°S volcanic zone, the SVZ is generally shallower than 2,300 mbsl but has a higher density of small volcanic cones (<2 km in width) and volcanic fissures around a central large volcanic edifice, the Starfish Volcano (~7.5 km wide) at about 12.2°S. The SVZ is the eastward continuation of the volcanic corridor that extends from the Tikopia Fracture Zone. South of the SVZ, the seafloor again deepens and the morphology transitions into the southern reaches of the DHGD and the VTT. The VTT exhibits a prevalence of N-S-trending lineament on its eastern and western flanks, which parallels lineaments in the JCT. A notable asymmetry is revealed by a relatively steep footwall scarp (rising up to 2,500 mbsl) forming the eastern boundary of the VTT and a gentler slope with diffuse faulting characterizing the arc-backarc transition to the west.

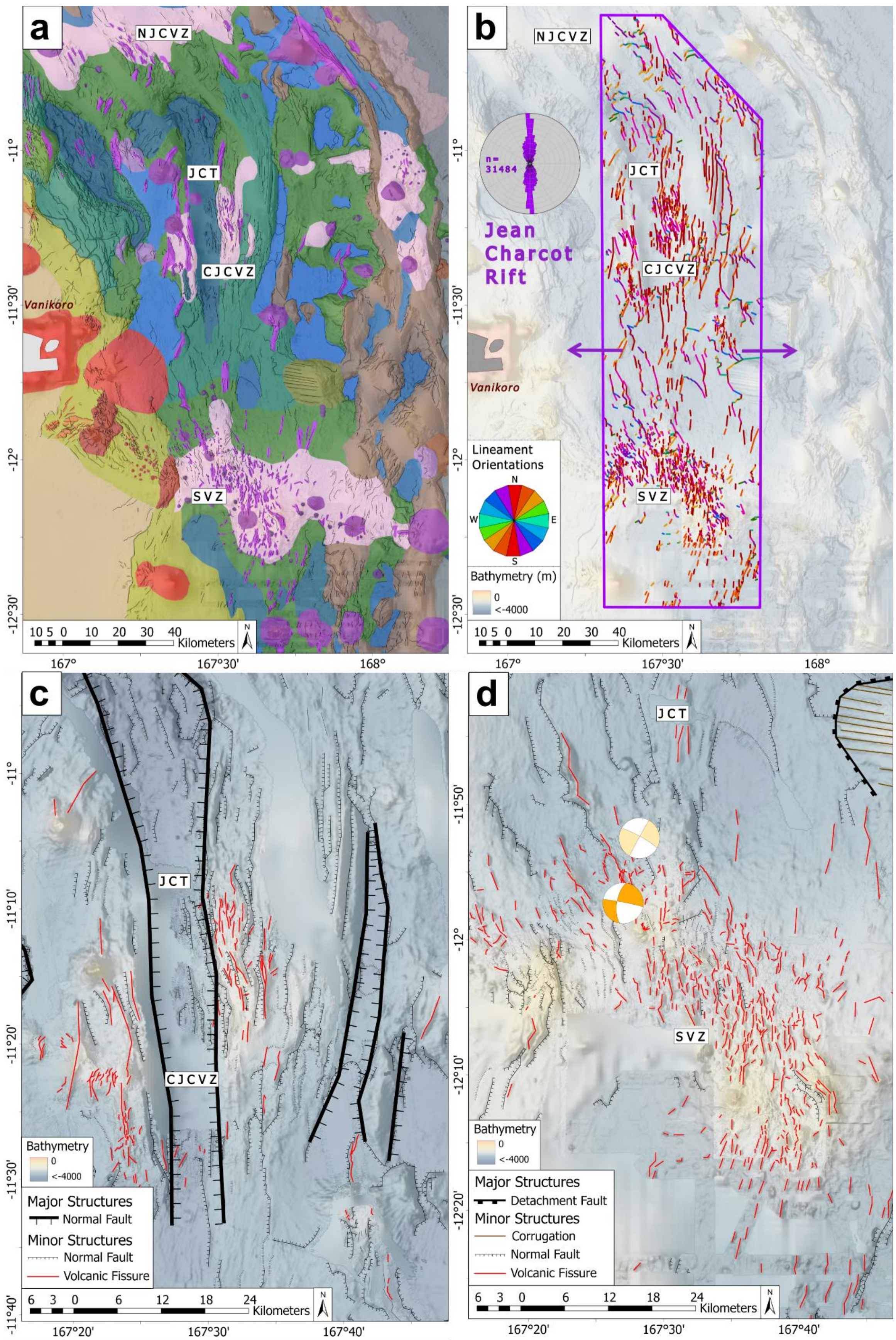
a
NJCVZ
JCT
CJCVZ
SVZ
Vanikoro
b
Jean
Charcot
Rift
n=
31484
Lineament
Orientations
Bathymetry (m)
0
<-4000
c
d
Bathymetry
Major Structures
Normal Fault
Minor Structures
Volcanic Fissure
Detachment Fault
Corrugation
Kilometers
-11°
-11°30'
-12°
-12°30'
167°
167°30'
168°
-11°10'
-11°20'
-11°40'
167°20'
167°40'
-11°50'
-12°10'
-12°20'

375

Figure 7: A) Morphotectonic map of the Jean Charcot Rift; B) Lineament orientation map of the Jean Charcot Rift. Purple arrows indicate the east-west extension interpreted from the uniformity of north-south trending lineaments; C) Structural map of the Central Jean Charcot Volcanic Zone. A symmetrical rift valley with a hummocky floor separates the the volcanic field. A rift valley to the east has a sedimented valley floor suggesting formed earlier than rifted volcanic field and westward migration of the rift axis; D) Structural map of the Starfish Volcanic Zone. Prolific volcanism is indicated by a high density of volcanic cones and fissures and shallow bathymetry relative to the deeper regions to the north and south where volcanic features are sparse. Acronym meanings are provided in Figure 2 caption.

4.2.2 Northwestern backarc rifts: The Santa Cruz Troughs

The SCT is a backarc domain that is characterized by abundant young hummocky volcanic flows and active seismicity (**Fig. 8a**). The SCT is bound by the RIP to the north, the arc-backarc transition to the southwest, and the 11.3°S and 10.6°S volcanic zones to the east. The 10.6°S volcanic zone extends into the northern-most trough within the SCT with rifted volcanoes and volcanic fissures occurring at greater depths. This domain is characterized by NW-SE to NNW-SSE striking normal dip slip to right lateral oblique slip fault kinematics with two peak orientations at 145–150° and 160–165° (**Fig. 8b**). Directly south of the Nendö Fault is the northernmost trough in this domain, the north SCT (**Fig. 8c**). This trough deepens towards the north where a maximum depth of ~3,700 m is reached at the footwall of the Nendö Fault. It has a hummocky and heavily faulted morphology populated with numerous volcanic fissures and rifted volcanic edifices. The southeastern end of this domain features another trough, a ~65 km long, ~20 km wide sigmoidal-shaped trough with a maximum depth of ~4,000 m at its north end (**Fig. 8d**). The morphology of this trough is characteristic of transtensional troughs (cf. Wu et al. 2009) with the following notable observations: 1) the trough footwall scarps can be observed on either side of the basin with a maximum throw of ~1,700 m on the eastern flank and ~2,600 m on the western flank; 2) along the trough axis, trending NNW-SSE, a discontinuous ridgeline represents the cross-basin strike-slip zone; and 3) extending south from the western basin footwall, the escarpment fans out into a series of en echelon normal faults that parallel the cross-basin ridge. Southwest of the trough, a sequence of parallel NNW-SSE-trending faults produce a terraced morphology, stepping up towards the arc-backarc transition. On the eastern bounding horst, a bathymetric peak depicts the morphology of a rifted volcano.

407

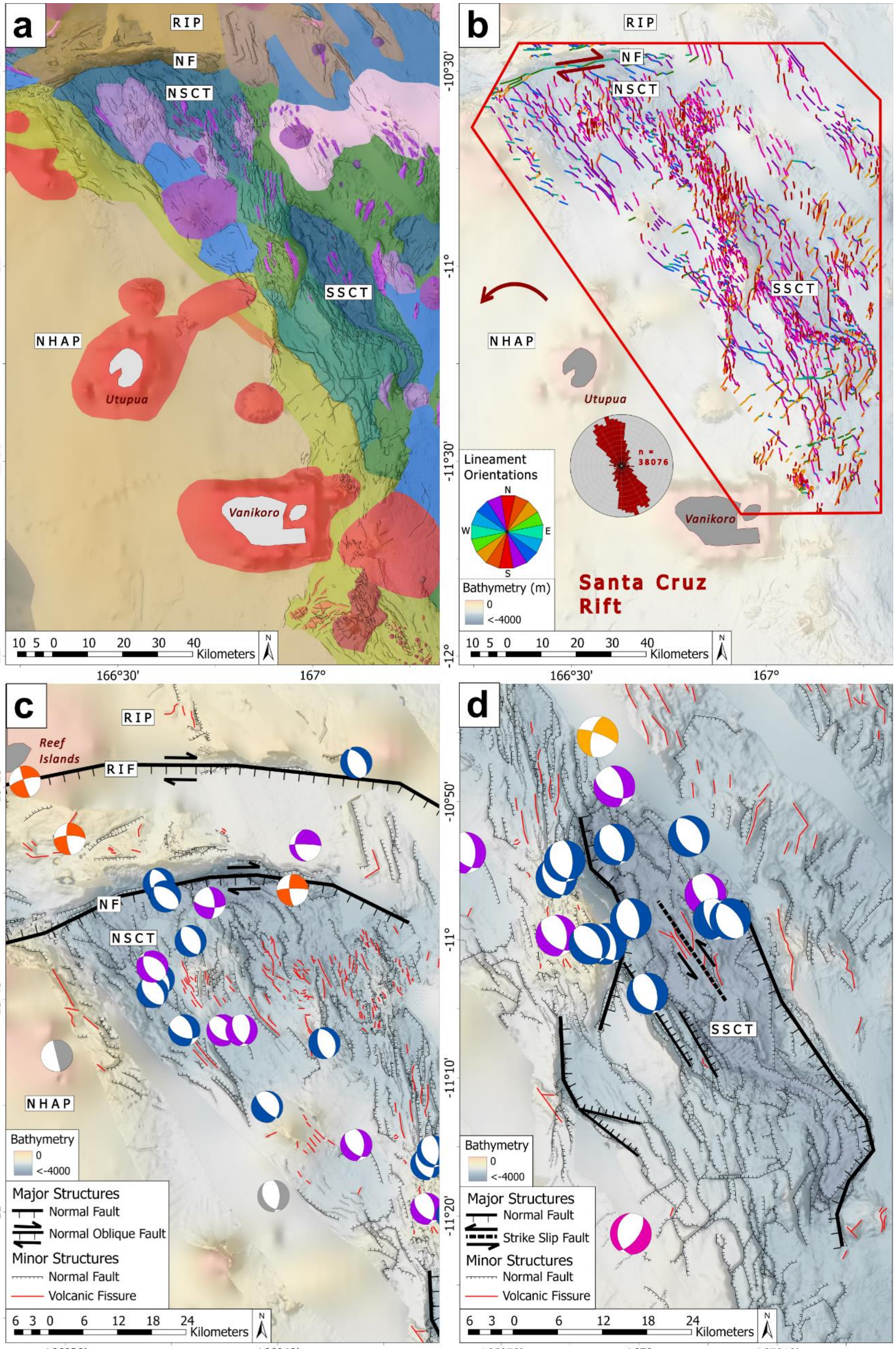
a
RIP
NF
NSCT
SSCT
NHAP
Utupua
Vanikoro
-10°30'
-11°
-11°30'
-12°
166°30'
167°
10 5 0 10 20 30 40 Kilometers
b
RIP
NF
NSCT
SSCT
NHAP
Utupua
Vanikoro
n = 38076
Lineament Orientations
N
E
S
W
Bathymetry (m)
0
<-4000
Santa Cruz Rift
c
RIP
Reef Islands
RIF
NF
NSCT
NHAP
-10°20'
-10°40'
-11°
166°20'
166°40'
Bathymetry
Major Structures
Normal Fault
Normal Oblique Fault
Minor Structures
Volcanic Fissure
6 3 0 6 12 18 24 Kilometers
d
SSCT
-10°50'
-11°10'
-11°20'
166°50'
167°10'
Strike Slip Fault

Figure 8: A) Morphotectonic map of the Santa Cruz Rift; B) Lineament orientation map of the Santa Cruz Rift. Red double arrows indicate dextral fault kinematics along the Nendö Fault. Curved arrow indicates counterclockwise rotation of the New Hebrides Arc Platform; C) Structural map of the North Santa Cruz Trough and south Reef Islands Platform. Normal to normal-oblique fault kinematics indicated active extension in the South Santa Cruz Trough accomodating southwestward migration of the North New Hebrides Arc. Two crustal-scale faults, the Reef Islands Fault and the Nendö Fault, accommodate dextral motion between the Reef Islands Platform and the North New Hebrides Arc; D) Structural map of the south Santa Cruz Trough. The morphology of the trough is characteristic of a transtensional pull-apart basin: footwall uplifts on both sides of the trough are assymetrical in relation to a cross-basin high, which represents an axial strike slip zone; an en-echelon ramp relay trails the eastern footwall uplift. A rifted volcano is a likely source of weakness where rifting initiated. CMT classifications provided in Figure 3. Acronym meanings provided in Figure 2 caption.

4.3 The arc-backarc transition, the arc, and the forearc

The arc-backarc transition is a 5–40 km wide zone to the west of the backarc troughs and forms the slope that rises to the arc platform (**Fig. 2**). This zone hosts numerous arc volcanoes and is characterized by a faulted morphology. Fault trends generally parallel lineament orientations in the neighbouring backarc. Two rifted volcanoes are located within the transition zone, one at~12°S and one at ~12.8°S. The 12°S volcano is west of the SVZ and is rifted in a WNW-ESE direction with the two halves separated by a ~20 km trough that is populated by numerous small volcanic cones and fissures. The 12.8° trough is west of the VTT and is actively rifting as indicated by three local CMTs interpreted with normal to normal-left lateral oblique slip fault kinematics. The volcano is rifted in a NNW-SSE direction with the two halves separated by a ~10 km trough. The extension direction exhibited within these troughs contrasts with the general E-W extension in the neighbouring SVZ and VTT, respectively.

The NHA Platform is 40–90 km in wide and is characterized by a smooth, flat-topped morphology and thick sedimentary deposition (Charvis and Pelletier, 1989). The region is undeformed with the exception of the northernmost region of the platform where an ENE-WSW belt of seismicity extends from the

Nendö fault and through the island of Nendö. Nendö and two additional islands, Utupua and Vanikoro, constitute the Santa Cruz islands.

The north New Hebrides Forearc is 50–80 km wide and slopes down from the arc platform to the New Hebrides Trench, where a maximum depth of >9000 m is reached at ~11.9°S. A single forearc uplift (the Torres Islands) occurs between ~12.6–13.7°S. Viewed in reference to the trench axis, the forearc uplift lies directly opposite from the WTM on the subducting Santa Cruz Basin.

5 Discussion: Spatio-temporal phases of backarc opening

The culmination of mapping outcomes, including geologic and structural mapping, relative age relationships, zonal variations of lineament orientations, and fault kinematics inform on an interpretation of this complicated spatio-temporal history of backarc basin opening within the NHSZ. We identify three specific phases of rifting, constrained by previously established regional tectonic events. The three phases include: 1) rifting of the relict arc associated with the cessation of seafloor spreading in the northwest NFB, arc collision with the DER, slab rollback, and continued clockwise rotation of the arc, 2) E-W-directed rifting, primarily in the JCT, associated with the New Hebrides backarc basin formation with continued slab rollback, and a transition in arc rotation, and 3) NE-SW directed rifting in the SCT associated with the arrival of the WTM at the New Hebrides Trench, counterclockwise rotation of the arc, and the formation of a microplate boundary with the RIP to the north.

5.1 Rifting of the relict arc

The initiation of backarc rifting begins with the rifting of the relict New Hebrides Arc, represented by the Duff Troughs in the north, separating the DR and the RIP, and the DHGD in the east. The northern and eastern rifts exhibit distinct seafloor morphologies and dissimilar patterns in seafloor fabric therefore we classify these regions as distinct domains and interpret them separately below.

5.1.1 Phase one: Rifting of the DHGD and clockwise rotation of the north New Hebrides Arc

The presence of two lineament orientation peaks in the DHGD combined with laterally offset horst ridgelines observed in the morphology indicates a transtensional stress regime with conjugate normal to oblique-strike slip faulting (**Fig. 6**). The change to prevalent NE-SW-trending structures and the presence of a ~25 km hummocky-bottomed basin at the southeastern corner of this domain is likely the result of influences from spreading occurring near the backarc-Hazel Holme Fracture Zone intersection. The initiation of rifting within the arc can be explained by events occurring within the neighbouring NFB. The orientation of magnetic lineations indicate NE-SW-directed spreading in the northwest NFB up until ~7 Ma, accommodating clockwise rotation of the arc (Pelletier et al., 1993; Auzende et al. 1995). This was followed by N-S-directed spreading along two paleo-spreading centres (the Tikopea and Hazel Holme Fracture Zones) up until ~3 Ma (Pelletier et al., 1993; Auzende et al. 1995). It is conceivable that dextral motion and/or oblique spreading along these fracture zones continued to accommodate clockwise rotation of the arc during this period. After ~4 Ma, two tectonic events likely contributed to the commencement of arc rifting in the northern NHA. The first is related to the opening of the Lau Basin to the east by ~3 Ma, which resulted in stress field changes and a second reorientation the NFB spreading axes (Auzende et al., 1995). At this time, E-W directed spreading began in the southern NFB near 173°E as far north as ~15°S in the NFB (Pelletier et al., 1993; Auzende et al. 1995). North of the Hazel Holme Fracture Zone, seafloor spreading ceased. The second event is the collision of the DER by ~3–2 Ma, which resulted in compressional tectonics in the central segment of the subduction zone (Macfarlane et al., 1988; Greene et al., 1994). Dating of arc volcanic rocks indicate that volcanism on the eastern ridges of the DHGD and the western ridgeline bounding the VTT ended by ~3.5 Ma and 2.7 Ma, respectively

(Maillet et al., 1995), and provides a minimum constraint on the period of arc rifting. Eastward thrusting in the central portion of the subduction zone together with ongoing slab rollback to the north, segmented the arc (Greene et al., 1994; Pelletier et al., 1998; Calmant et al., 2003) and reversal of the kinematics of the Hazel Holme Fracture Zone from dextral to sinistral motion is required to explain the displacement caused by compression to the south. An E-W alignment of shallow strike-slip earthquake focal mechanisms have been interpreted to be a sinistral transform boundary between the north and central arc segments (Taylor, 1995). With the absence of seafloor spreading north of the Hazel Holme Fracture Zone and the initiation of E-W sinistral motion along the Hazel Holme Fracture Zone, rifting in the northern NHA was required to continue to accommodate asymmetric rollback of the subducting Santa Cruz Basin and continued clockwise rotation of the northern arc segment. The rifting of the arc produced the DHGD as revealed by the indicators for transtensional deformation; namely, two peak lineament orientations trending N-S and NNE-SSW, offset horsts, and the wedge shape of the DHGD (widening from north to south). This interpretation supports the continuation of the pre-rift clockwise rotation of the northern arc segment.

5.1.2 Phase one: Rifting of the Reef Islands Platform from the Duff Ridge

Given the positions of the RIP and DR relative to the active NHA—indicating dextral displacement along the Nendö Fault—we interpret that a single coherent arc platform existed during most of the earlier ~10-3 Ma clockwise rotation of the arc (Falvey, 1978; Musgrave and Firth, 1999). During this time, the northern portion of the arc platform translated away from a position above the subducting slab, as demarcated by the Santa Cruz Transform Fault as depicted in **Figure 1**. The rifting of the relict arc north of the Nendö Fault, represented by the North and South DT, likely occurred sometime after ~7 Ma in response to a change from NE-SW- to N-S-directed rifting in the northwest NFB as revealed by magnetic lineation data (Auzende et al., 1995). However, the exact timing is unclear; rifting may have occurred during rifting within the DHGD and clockwise arc rotation or later during the initiation of counterclockwise arc rotation in response to arc collision with the DER and the coeval cessation of seafloor spreading in the northwest NFB ~3 Ma (Greene et al., 1994; Auzende et al., 1995). In either case, continued rollback of the Santa Cruz Basin likely induced rifting of the northern arc segment and opening of these two troughs, prior to the detachment of the RIP from the active arc further south.

Lineament analysis of the north DT indicates two peak lineament orientations, one trending 85–90° and another trending 105–110° (**Fig. 4b**). While this may indicate a transtensional component to basin spreading, it is observed that the 105–110° lineaments are found predominantly in the smaller, shallower basin to the south. The lineament fabric in this lesser basin connects to the south DT indicating that the two are structurally related (**Figs. 4c** and **4d**). The contrast in lineament orientations between the north DT and the south DT with its northern continuation may indicated that the two troughs may have opened in sequence under changing stress regimes (i.e., the opening of the north DT preceded that of the south DT). The steep escarpment bounding the south DT to the east and the gently sloped RIP to the west is characteristic of a rollover anticline forming through extension along a low-angle detachment fault with a listric geometry (c.f., Dula, 1991). Prior to rifting, the coupled RIP-DR arc-front would have been level. The initiation of extension in the south DT caused the formation of a detachment fault dividing the DR and RIP and projecting beneath the RIP, which rifted southwest relative to the DR. During this rifting, the eastern RIP subsided, creating the gently sloped morphology.

The morphology and lineament orientation of the two northern troughs contrasts sharply with the more complex domains to the south of the Reef Islands and Nendö Faults. The relative timing of the northern troughs with respect to the rifting and basin opening to south can be constrained by noting that the north and south DT contain heavily sedimented basin floors, while backarc rifting in the JCT is hummocky, indicating relatively recent volcanism in the latter. The opening of the northern troughs therefore occurred sometime before the extensional phase of opening in the JCT. We further interpret that the rupture of the Reef Islands and Nendö Faults caused the cessation of rifting north of this microplate boundary.

5.2 Phase two: Rifting of the Jean Charcot Troughs and transitional arc rotation

The JCT is a ~40 km wide zone of E-W extension that stretches N-S for ~150 km and is bisected by the 10.6°S volcanic zone to the north and the SVZ centred at 12.1°S. The JCT is interpreted to be a failed rift—a diffuse zone of extension in which a spreading axes fails to materialize—based on backarc basin basalt (BABB) geochemical signatures of dredged seafloor samples from the SVZ (Monjaret et al., 1991; Maillet et al., 1995). Geologic interpretations and the lineament analysis in this study support the failed rift interpretation. Within the JCT, abundant volcanic fissures within the 11.3°S volcanic zone and the SVZ and normal faulting more broadly, share a remarkably uniform N-S orientation and indicate a period E-W-directed extension (**Fig. 6b**). The morphology of the 11.3°S volcanic zone—a deep axial graben with a hummocky floor and steep valley walls with high relief—is characteristic of a slow-spreading centre (**Fig. 6c**). We interpret this observation as the establishment of an incipient spreading centre near the end of the diffuse rifting period. In total, the extension in the JCT resulted in up to ~60 km of extension in the backarc along a length of ~180 km. Dredged backarc basin basalt samples from the SVZ were dated to have erupted between ~2.7–1.1 Ma, placing upper and lower constraints on the opening of the JCT (Monjaret et al, 1991; Maillet et al., 1995). This extensional period was likely accommodated along E-W oriented structures located within and obscured by younger volcanic flows in the 10.6°S volcanic zone in the north and the SVZ in the south.

To the south of the SVZ, a single ~110 km long graben, the VTT, bears morphological similarity to the south DT in having a steep escarpment on its eastern margin, contrasting with a gently sloped, though faulted margin along the arc/backarc transition (**Fig. 6d**). The VTT may represent the initiation of a detachment fault coeval with the beginning of extension in the JCT. Rifting south of the SVZ is interrupted early in the initial extensional phase as compared to the JCT, and the VTT reached a maximum width of only <10 km. A possible explanation for this early interruption may be the nearing of the West Torres Massif on the subducting plate prior to its arrival 1.0–0.7 Ma (Meffre and Crawford, 2001) and the ceasing of slab rollback south of ~12°S. Continued rollback north of ~12°S allowed for continued backarc extension in the JCT and accommodated along E-W transform faults within the SVZ.

5.3 Transition from extensional to transtensional rifting

The morphological arrangement of the JCT, the south SCT to the west, and the region between them bear a remarkable resemblance to that described by Auzende et. al (1988) in a region to west of the Fiji archipelago. The authors describe a region with two sub-parallel N-S-oriented grabens separated in the north by a shallower subsidiary trough with dominant lineament fabric at a ~25° obliquity to the N-trending grabens, and in the south by a plateau with complex arcuate structures (Fig. 16 in Auzende, et al., 1988). Auzende et al. (1988) interpret the structures as resulting from dextral regional deformation, perpendicular to the sinistral North Fiji Fracture Zone, contributing to counterclockwise rotation of the Fiji platform. In our model, we propose that this morphology and the spatial relationship of the lineament fabric represents a period of transition from extensional to transtensional rifting (**Fig. 9**). Four key observations support this: 1) The SCT is seismically active and therefore likely opened after the opening of the JCT, which is seismically inactive; 2) a change in peak lineament orientation frequencies from a N-S trend in the JCT to paired NW-SE/NNW-SSE trends in the SCT; 3) N-S trending faults (associated with E-W extension in the JCT) are seen to be crosscut by NW-SE and NNW-SSE trending faults (associated with NE-SW- and ENE-WSW-directed extension in the SCT) in areas where high resolution (25 m) bathymetry is available on the arc/backarc transition southeast of the island of Vanikoro (**Fig. 10a**) and in the north SCT (**Fig. 10b**); and 4) the contrast between the slow-spreading centre morphology in the central JCT and the pull-apart basin morphology of the neighbouring south SCT. In addition, the plateau between the two N-S grabens west of Fiji are interpreted to have arcuate structures as a result of intra-plate rotation during the opening of the two troughs. The region between the transtensional south SCT and extension JCT is relatively undeformed, supporting episodic rather than simultaneous opening of the two troughs.

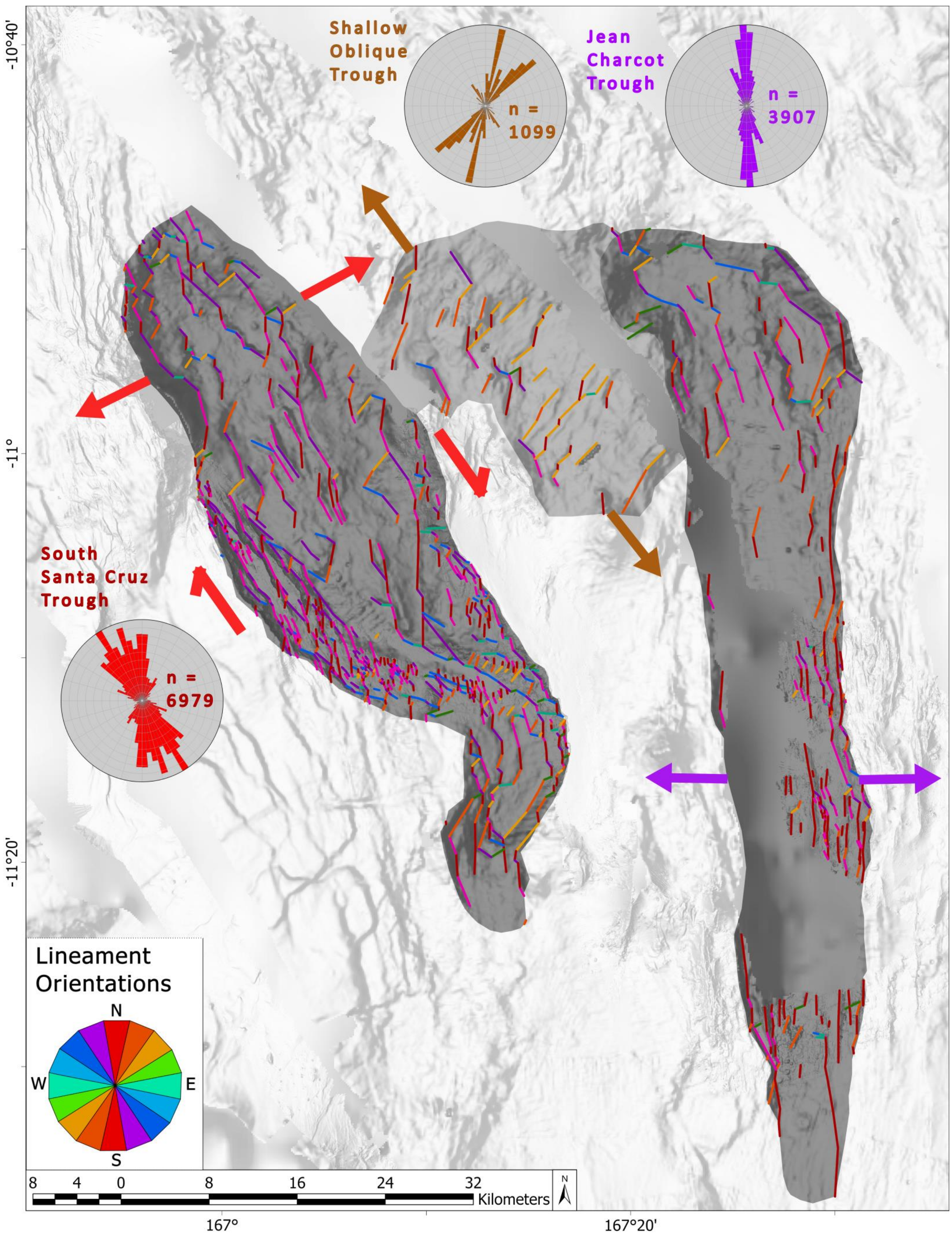

Figure 9: Interpreted sequential opening of the Jean Charcot Trough and the South Santa Cruz Trough. The JCT opened during an earlier stage of rifting characterized by E-W extension. The south SCT opened later through transtensional opening characterized by NNW-SSE extension accompanied by

dextral motion along a central trough axis. The two troughs are bridged by a lesser, shallower trough with an extension direction oblique to both troughs.

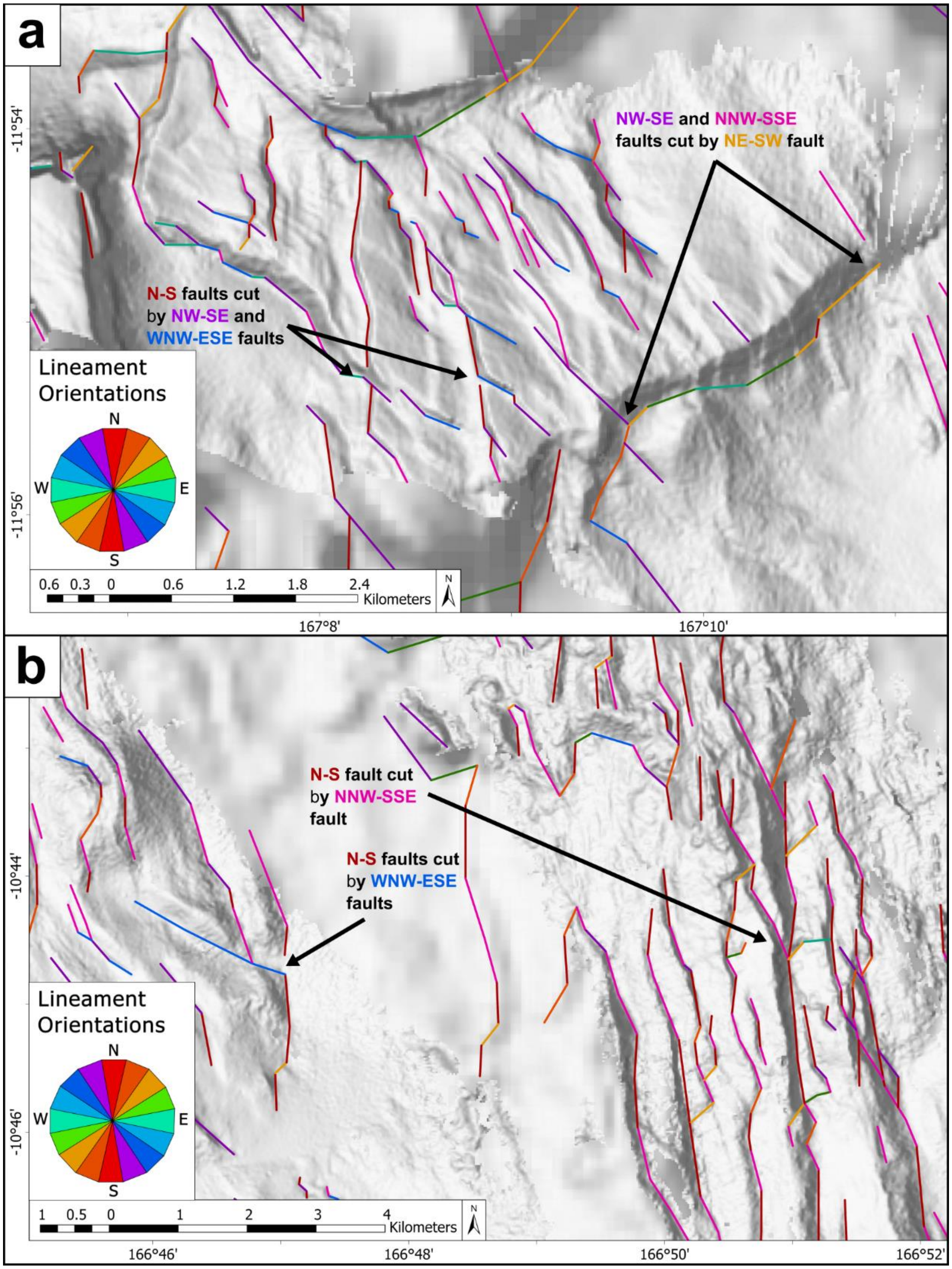

Figure 10: a) Faulted morphology in the New Hebrides arc/backarc transition. N-S trending faults reveal the western most extent of the Jean Charcot Rift. NW-SE trending faults associated with the Santa Cruz Rift crosscut N-S trending faults. NW-SE trending faults are themselves crosscut by conjugate NE-SW trending faults also associated with the Santa Cruz Rift; b) Faulted morphology in the Kaiyo Trough. N-S trending fault in the east of the area are crosscut by NNW-SSE trending fault, indicating that N-S trending structures in the South Santa Cruz Trough may have formed during the Jean Charcot stage of rifting and were later crosscut by ENE-WSW extension during the Santa Cruz stage of rifting. In the west of the South Santa Trough, N-S trending fabric is sparser and the dominant fabric trends NW-SE. Here, a N-S trending structure is crosscut by a WNW-ESE fault.

The presence of a subsidiary basin with ~25° obliquity to, and lying between the two primary troughs, in both the NFB (Auzende et. al, 1988) and northern NHB is a noteworthy observation. Considering the scenario in this study—episodic rifting in a nascent backarc basin—the oblique structural fabric trending NE-SW in the arc-backarc transitional zone may be the antecedent to the opening of subsidiary basins oblique to the prevalent seafloor fabric in adjacent backarc troughs. Three such regions of structural obliquity are observed on the arc-backarc transition. The first is between the south end of the south SCT and an arc volcano to the west (~167°S, 11.3°S; **Fig. 7b**). Here, NE-SW trending structures intersect with the predominant NW-SE- to NNW-SSE-trending structures, which produce the terraced morphology of the area. A single CMT in this zone reveals right-lateral oblique dip-slip fault kinematics with a strike that is ~45° oblique to the dominant fault slip trends in the south SCT. The second is the 12°S rifted volcano the arc-backarc transition where NE-SW faults crosscut the prevalent NW-SE and NNW-SSE seafloor fabric (167.2°E, 12°S; **Fig. 8a**). The third is the 12.8°S rifted volcano on arc backarc transition; both rifted volcanoes form young, faulted troughs with orientations oblique to the neighbouring backarc troughs (**Fig. 7a**). The presence of oblique seafloor fabric and/or relatively shallow subsidiary basins is interpreted to be a feature of strain partitioning either between actively opening troughs (e.g., Auzende et al., 1988), or in a transition period during which there is a jump in the locus of basin opening (this study).

5.4 Phase three: Arrival of the West Torres Massif, counterclockwise arc rotation, and rifting of the Santa Cruz Troughs

The seismically active SCT represents the most recent shift in tectonic stresses. The pull-apart basin morphology of the south SCT, the normal dip slip to normal right lateral oblique slip fault kinematics, and dual peak lineament orientations indicate a change from E-W-directed extension (JCT) to NNE-SSW and NE-SW-directed transtensional to extensional rifting within the SCT. This transition is interpreted to be the result of the arrival of the WTM at the NHT at ~0.7–1.0 Ma (**Fig. 1**; (Meffre and Crawford, 2001). Incipient compressional tectonics inboard of the trench between 13–15°S is evidenced by forearc uplift (i.e., West Torres Islands; Calmant et al. 2003) and may explain discontinuation of rifting in the JCT. Though no volcanic samples have been dated in the SCT, the end of backarc volcanism in the JCT by ~1.1 Ma (Monjaret et al, 1991; Maillet et al., 1995) constrains the transition in location of backarc rifting and agrees with the timing of the arrival of the WTM. Arrival of the WTM likely caused emplacement of a rotation hinge point in the northern NHA with a pole of rotation just south of the SVZ as determined Bergeot et al. (2009) and Calmant et al. (2003) using GPS velocity data. Current convergence rates at the north end of the northern NHSZ are ~150–170 mm/yr, with ongoing slab retreat being accommodated by ~80 mm/yr of backarc extension (Calmant et al. 2003). The asymmetry in convergence caused by compression induced by the arc-plateau collision in the south and slab retreat in the north can explain the counterclockwise rotation of the arc platform and the ongoing rifting in the SCT.

A network of arcuate normal faulting to the south of the south DT mimic the larger arcuate geometry of the of the north and south DT. Arcuate faulting patterns are characteristic features resulting from strain partitioning near crustal-scale transform boundaries and have been described in both extensional (e.g. Owen Fracture Zone, NW Indian Ocean: Rodriguez et al., 2013) and compressional tectonic settings (e.g.

Altyn Tagh Fault, Himalayan Plateau: Dupont-Nivet et al., 2004). It is likely, therefore that the arcuate faulting pattern south of the south DT was a precursor to the full crustal-scale rupture that formed the Reef Islands and Nendö Faults and the consequent dismemberment of the RIP from northern NHA crustal block (**Fig. 5d**). The timing of the initial crustal-scale rupture is likely to have been caused by the arrival of the WTM as interpreted from the asymmetry of convergence along the northern NHA, the emplacement of a hinge of counterclockwise rotation within the northern NHA, the initiation of rifting that formed the SCT, and the lack of slab suction (the northern slab edge being roughly in alignment with the Santa Cruz Transform Boundary to the west; Neely and Furlong, 2018).

6 Discussion: Controls on the distribution of volcanism across the New Hebrides Backarc

Within the NHB, we identify two volcanic corridors that span the width of the backarc: the 10.6°S volcanic zone (**Fig. 5a**) and the SVZ (**Fig. 6a**). Both zones feature hummocky terrains and a high density of volcanic cones and fissures, rise up to more than 1 km above the surrounding seafloor (interpreted to be magma deficient areas), are elongated in an orientation roughly perpendicular to the arc, and are preserved through all phases of backarc opening. Within the spatio-temporal framework of basin opening, we infer that volcanism progressed from east to west with progressive westward arc migration. In this scenario, the conduits for backarc volcanism may be inherited from the rifting of arc volcanoes that then migrate trenchward. Karig (1970) demonstrates the proto-Kermadec Arc was the locus of rifting that produced the Havre Trough and effectively split the arc into the relict Lau Arc and the active Kermadec Arc. Molnar and Atwater (1978) further explain that arc volcanoes may act as points of weakness and preferentially control where rift initiation begins. This is supported by this study with the observation that a number of relict intra-arc troughs (167.8°E, 10.6°S on **Fig. 5a**; 168.2°E, 12.0°S on **Fig. 6a**) and backarc troughs (167.8°E, 10.7°S; 167.2°E, 11.3°S on **Fig. 8a**) exhibit rifted volcano morphologies on their footwall escarpments. Two rifted arc volcanoes are also observed on the arc-backarc transition (167.2° E, 12.0°S; 167.4°E, 12.8°S on **Fig. 6a**). Jumps in the axis of rifting and associated changes in relative plate motions, as observed with MOR spreading centres, are also plausible in backarc basins, with migrating arc volcanoes repeatedly acting as centres for rifting (Molnar and Atwater, 1978). Wright et al. (1996) interpret a series of "cross-arc ridges" that interrupt the continuity of the Havre Trough in the Kermadec Subduction Zone as composites of "arc massifs" produced by the migration of arc volcanoes, most notably The Rumble V Ridge, which has dimensions and relative depths very similar to the volcanic corridors described in this study. While this is a reasonable interpretation for the formation of voluminous tracts of volcanism, this does not explain why not all arc volcanoes form corridors of prolific volcanism.

Alternatively, the continuity of the volcanism in the SVZ and 10.6°S volcanic zone may have formed along pre-existing crustal-scale structures, which track behind arc migration and enables concentrated backarc volcanism. In the case of the Rumble V corridor, Wright et al. (1996) suggested that it is possible (though unlikely in their study area) that underlying transform faults or pre-existing arc discontinuities may have promoted greater volumes of volcanism. Specific to the NHB, however, Anderson et al. (2016) observed that the volcanic terrain of the SVZ tracks from the intersection of the relict arc with the Tikopia Fracture Zone in the NFB, a sequence of deep, E-W oriented troughs that exhibit the morphology of an ultraslow spreading centre. The Tikopia Fracture Zone is seismically inactive, however, and an alternative mechanism is required to account for structural continuity. The width of the JCT to the north of the SVZ (~80–100 km) is notably greater than the width of the backarc directly to the south (~10–50 km), particularly in the VTT, this can partly be explained by transform faulting beneath the volcanic strata of the SVZ inheriting the E-W-trending rupture planes of the Tikopia Fracture Zone normal faults. These transform faults may then also function as conduits for backarc volcanism. In the 10.6°S volcanic zone, a link between a crustal-scale structure and prolific volcanism is enigmatic. No major structure is observed in the adjacent NFB, however NW-SE-trending lineament orientations in the 10.6°S volcanic zone deviate from the N-S trending lineaments in the JCT to the south, indicating a deformation history that perhaps bridges E-W extension in the JCT to the south with arcuate faulting patterns and the eventual dismemberment of the RIP to the north (**Fig. 5a**). In our model, we propose that the combination of the two aforementioned processes—repeated rifting of and migration of arc volcanoes and crustal scale structures that track behind arc migration—are prerequisites for producing corridors with high volume volcanism.

7 Discussion: Implications for nascent backarc rifting processes

Many tectonic complexities influence the initiation and progression of backarc rifting including variations in slab dip angles (Lallemand et al., 2005; Sdrolia & Müller, 2006), slab tearing and associated subduction transform edge propagator fault formation (Lister et al., 2012; Neely and Furlong, 2018), asymmetric slab rollback (Schellart et al., 2002), and buoyant ridge-forearc collisions and associated arc segmentation and block rotations (Calmant et al., 2003; Bergeot et al., 2009; Wallace et al., 2009). In this study, we characterize the geodynamic character of backarc rifting in the north NHB which, being one of the world's youngest backarc basin and having been affected by several tectonic complexities preserves the earliest phases of backarc basin opening. We advance three important interpretations about early backarc rifting based on our observations of the New Hebrides Subduction Zone. First, the focal point of opening of intra-arc troughs occurs at arc volcanoes, consistent with the evidence first presented by Karig (1970) that extension in arc settings begin at arc volcanoes where thermal weakness in the crust is induced by arc plutonism. This is best supported by the 12°S and 12.8°S rifted volcanoes located on the arc-backarc transition (**Fig. 2**). The same principle applies to the opening of troughs in the already established backarc, as can be observed in the south SCT where the bounding horst structures exhibit the morphology of a rifted volcano (**Fig. 8d**). These observations confer that early intra-arc/ backarc rifting is initiated at volcanic edifices. Second, rifting of the arc proceeds along low-angle detachment faults that projects trench-ward, beneath the arc. The morphologies of the south DT (**Fig. 5d**) and the VTT (**Fig. 6d**) both support this interpretation; steep escarpments bound the troughs opposite from the arc platform and a gently sloped morphology on the arc platform are characteristic of asymmetrical rifting along a deep detachment fault. The presence of an OCC at 167.8°E, 11.8°S exposes the detachment fault along a section of the backarc that has experienced more advanced crustal thinning and further supports arc migration along detachment faults following a period of arc rifting. The presence of an OCC and a concomitant detachment fault to the east of the JCT and north of the Tikopia Fracture Zone is reminiscent of OCCs previously described on the inside corners of slow-spreading mid-ocean ridge-transform intersections and the integral role of detachment faults in crustal accretion in these locations (Ildefonse et al., 2007; Escartin et al. 2008; Li et al., 2014). Therefore, the presence of detachment faults and associate OCCs in a backarc setting act as a bridge between early rifting and the eventual establishment of stable seafloor spreading. Third, once rifting has achieved sufficient crustal thinning, as signalled by the OCC exposure, mantle upwelling induces a period of profuse, localized volcanism that is antecedent to the development of a spreading axis. The morphology of a slow spreading axis is preserved in the 11.3°S volcanic zone, which, in contrast to the volcanic corridors to the north and to the south, is a zone of focussed magmatism without any lateral continuity to indicated pre-existing structural controls.

8 Conclusions

This study demonstrates the polyphase nature of the initiation and early rifting of nascent backarc basins. The process begins with rifting of arc crust at zones of crustal weakness, often at arc volcanoes as evidenced by the observation of numerous rifted volcanic edifices and fissures in this study. Diffuse rifting of the thickened relict arc produces a horst and graben morphology, such as the DHGD, that yields to broader and deeper trough formations along consolidated detachment faults as crustal thinning proceeds, such as in the JCT. Profuse focused volcanism appears in the later stages of early rifting and signals the development of a seafloor spreading centre orthogonal to the extension direction of rifting. In the NHB, this process is preserved by the 11.3°S volcanic zone where a deep elongate trough bisects the volcanic zone. We propose that the first two phases of opening, arc rifting and backarc trough opening, are common processes in the early phases of backarc basin development. In the case of the NHB, the culmination of a stable spreading centre as observed in mature backarc basin was interrupted by arc collision with the West Torres Massif and an abrupt shift in the loci of rifting to the SCT, leaving a seismically quiescent aborted spreading centre. In contrast to the isolation of the 11.3°S volcanic zone, two other zones of shallow, hummocky terrains present as corridors of high-volume volcanism stretching from the relict arc to the active arc volcanoes. Not all arc volcanoes are trailed by a belt of shallow, volcanic terrains, therefore, we propose that in addition to progressive rifting of arc volcanoes and backarc inheritance of magma conduits, secondary deformation structures are required to account for the >1 km thick volcanic strata observed. In this study, we demonstrate that the opening of the New Hebrides Backarc and associated evolution in volcanism involved distinct spatio-temporal phases within the context of tectonic complexities which, being common in the evolution of other backarc basins, allows these new insights to be applied to our understanding of backarc basins more broadly.

Acknowledgements

MOA acknowledges funding from NSERC-DG, the NSERC-CREATE iMAGE grant, and the Connaught New Researcher program (UofT). This is contribution MERC-ME-2024-## to the modern-ancient crust project of the Canadian Metal Earth program.

Availability Statement

The creation of the remote-predictive geological and structural maps in this study incorporates open-sourced regional bathymetric data included in the GEBCO Compilation Group database (GEBCO 2023 Grid), available from https://doi.org/10.5285/1c44ce99-0a0d-5f4f-e063-7086abc0ea0f. Additional open-sourced bathymetric data used in this study include the MGL0904 cruise (Johnson; A., 2009), available on the Rolling Deck to Repository database from https://doi.org/10.7284/903749. Bathymetric data collected during the 1993 SOPACMAPS cruises were provided to us (GEOMAR) via a formal cooperative research agreement with IFREMER with metadata available through the French Oceanographic Campaigns database: https://doi.org/10.17600/93000250 (SOPACSMAPS.LEG1; Daniel, J., 1993), https://doi.org/10.17600/93000251 (SOPACSMAPS.LEG2; Auzende, J. M., 1993), https://doi.org/10.17600/93000252 (SOPACSMAPS.LEG3; Pelletier, B., 1993). To obtain this data, contact IFREMER (L. Petit de La Villéon: https://en.ifremer.fr/) to arrange a data sharing agreement. Finally, as this area has been poorly-explored by the scientific community, this study relies on additional bathymetric data from commercial partners through cooperative research agreements, and as such, the raw and processed data are not openly available to the public or researchers. This includes bathymetric data provided by Neptune Minerals, Inc. (recently acquired by Magellan), collected during the ASHR Leg 2 cruise in 2011 aboard the MV Dorado Discovery, covering 685.6 km^2 in the Starfish volcanic field (extent: N=12.0°S, E=167.7°E, S=12.3°S, W=167.3°E) at a resolution of 50 m. This bathymetric data is published in Anderson et al., 2019. To gain access, researchers can contact Magellan (https://www.magellan.gg) to initiate a formal agreement. Similarly, additional bathymetric data is provided by Nautilus Minerals, Inc. (now The Metals Company), collected during the DUKE15 cruise in 2015 (extent: N=9.2°S, E=167.89°E, S=12.1°S, W=165.6°E), at a 25 m resolution. To gain access, researchers can contact The Metals Company (https://metals.co/) to initiate a formal agreement. Centroid moment tensor data used in this study were acquired from the Global CMT Catalog (Dziewonski, A. M., 1981; Ekström, G., et al., 2012) and are accessible through their search engine, https://www.globalcmt.org/CMTsearch.html. Remote-predictive mapping was accomplished with ArcGIS Pro v.3.2.2 under an ESRI Inc. license available at https://www.esri.com/en-us/arcgis/products/arcgis-pro/overview. We would like to acknowledge Dr. Tiesheng Wu for the ArcBeachball tool v.2.2, which was used to import and image CMT data into ArcGIS Pro. Maps exported from ArcGIS Pro were edited in Inkscape v1.2.1, an open-sourced application available at https://inkscape.org/, for the production of the figures in this manuscript. The full dataset of maps generated in this study are available in an online repository (Summer, D., 2024) that can be https://doi.org/10.5281/zenodo.13844923.

References

Anderson, M. O., Hannington, M. D., Haase, K., Schwarz-Schampera, U., Augustin, N., McConachy, T. F., & Allen, K. (2016). Tectonic focusing of voluminous basaltic eruptions in magma-deficient backarc rifts. *Earth and Planetary Science Letters*, *440*, 43-55. https://doi.org/10.1016/j.epsl.2016.02.002

Anderson, M. O., Hannington, M. D., McConachy, T. F., Jamieson, J. W., Anders, M., Wienkenjohann, H., ... & Petersen, S. (2019). Mineralization and alteration of a modern seafloor massive sulfide deposit hosted in mafic volcaniclastic rocks. *Economic Geology*, *114*(5), 857-896. https://doi.org/10.5382/econgeo.4666

Auzende J. M., (1993). SOPACMAPS.LEG2 cruise, RV L'Atalante. https://doi.org/10.17600/93000251

Auzende, J. M., Honza, E., Boespflug, X., Deo, S., Eissen, J. P., Hashimoto, J., ... & Urabe, T. (1990). Active spreading and hydrothermalism in North Fiji Basin (SW Pacific). Results of Japanese French Cruise Kaiyo 87. *Marine geophysical research*, *12*, 269-283. https://doi.org/10.1007/BF02428198

Auzende J. M., Pelletier B., Eissen J.P., 1995. The North Fiji Basin geology, structure, and geodynamic evolution. In: Taylor, B. (Ed.) *Backarc Basins: Tectonics and Magmatism* (pp. 139-175). New York, NY: Plenum Press.

Auzende, J. M., Rissen, J. P., Lafoy, Y., Gente, P., & Charlou, J. L. (1988). Seafloor spreading in the north Fiji basin (Southwest Pacific). *Tectonophysics*, *146*(1-4), 317-352. https://doi.org/10.1016/0040-1951(88)90098-4

Baxter, A. T., Hannington, M. D., Stewart, M. S., Emberley, J. M., Breker, K., Krätschell, A., ... & Anderson, M. O. (2020). Shallow seismicity and the classification of structures in the Lau back-arc basin. *Geochemistry, Geophysics, Geosystems*, *21*(7), e2020GC008924. https://doi.org/10.1029/2020GC008924

Bergeot, N., Bouin, M. N., Diament, M., Pelletier, B., Régnier, M., Calmant, S., & Ballu, V. (2009). Horizontal and vertical interseismic velocity fields in the Vanuatu subduction zone from GPS measurements: Evidence for a central Vanuatu locked zone. *Journal of Geophysical Research: Solid Earth*, *114*(B6). https://doi.org/10.1029/2007JB005249

Calmant, S., Pelletier, B., Lebellegard, P., Bevis, M., Taylor, F. W., & Phillips, D. A. (2003). New insights on the tectonics along the New Hebrides subduction zone based on GPS results. *Journal of Geophysical Research: Solid Earth*, *108*(B6). https://doi.org/10.1029/2001JB000644

Caratori Tontini, F., Bassett, D., de Ronde, C. E., Timm, C., & Wysoczanski, R. (2019). Early evolution of a young back-arc basin in the Havre Trough. *Nature Geoscience*, *12*(10), 856-862. https://doi.org/10.1038/s41561-019-0439-y

Charvis, P., & Pelletier, B. (1989). The northern New Hebrides back-arc troughs: history and relation with the North Fiji basin. *Tectonophysics*, *170*(3-4), 259-277. https://doi.org/10.1016/0040-1951(89)90275-8

Crook, K. A., & Belbin, L. (1978). The southwest Pacific area during the last 90 million years. *Journal of the Geological Society of Australia*, *25*(1-2), 23-40. https://doi.org/10.1080/00167617808729012

Crowhurst, P. (2015). DUKE 15 cruise, MV Duke.

Daniel, J., (1993). SOPACMAPS LEG1 cruise, RV L'Atalante. https://doi.org/10.17600/93000250

Dula Jr, W. F. (1991). Geometric models of listric normal faults and rollover folds (1). *AAPG bulletin*, *75*(10), 1609-1625. https://doi.org/10.1306/0C9B29B1-1710-11D7-8645000102C1865D

Dunn, R. A., & Martinez, F. (2011). Contrasting crustal production and rapid mantle transitions beneath back-arc ridges. *Nature*, *469*(7329), 198-202. https://doi.org/10.1038/nature09690

Dupont-Nivet, G., Robinson, D., Butler, R. F., Yin, A., & Melosh, H. J. (2004). Concentration of crustal displacement along a weak Altyn Tagh fault: Evidence from paleomagnetism of the northern Tibetan Plateau. *Tectonics*, *23*(1). https://doi.org/10.1029/2002TC001397

Dziewonski, A. M., Chou, T. A., & Woodhouse, J. H. (1981). Determination of earthquake source parameters from waveform data for studies of global and regional seismicity. *Journal of Geophysical Research: Solid Earth*, *86*(B4), 2825-2852. https://doi.org/10.1029/JB086iB04p02825

Ekström, G., Nettles, M., & Dziewoński, A. M. (2012). The global CMT project 2004–2010: Centroid-moment tensors for 13,017 earthquakes. *Physics of the Earth and Planetary Interiors*, *200*, 1-9. https://doi.org/10.1016/j.pepi.2012.04.002

Escartín, J., Smith, D. K., Cann, J., Schouten, H., Langmuir, C. H., & Escrig, S. (2008). Central role of detachment faults in accretion of slow-spreading oceanic lithosphere. *Nature*, *455*(7214), 790-794. https://doi.org/10.1038/nature07333

Falvey, D. (1975). Part 2. Younger Pacifics arcs and the eastern marginal seas: Arc reversals, and a tectonic model for the North Fiji Basin. *Exploration Geophysics*, *6*(3), 47-49. https://doi.org/10.1071/EG975047

Falvey, D. A. (1978). Analysis of palaeomagnetic data from the New Hebrides. *Exploration Geophysics*, *9*(3), 117-123. https://doi.org/10.1071/EG978117

GEBCO Compilation Group (2023). GEBCO_2023 Grid.

Greene, H. G., Collot, J. Y., Fisher, M. A., & Crawford, A. J. (1994). Neogene tectonic evolution of the New Hebrides island arc: A review incorporating ODP drilling results. In *Proceedings of the Ocean Drilling Program, Scientific Results* (Vol. 134, No. 1, pp. 19-46). College Station, TX: Ocean Drilling Program.

Hannington, M. D., De Ronde, C. E., & Petersen, S. (2005). Sea-floor tectonics and submarine hydrothermal systems. In: Hedenquist J. W., et al. (Eds.), *One Hundredth Anniversary Volume Economic Geology* (pp. 111-141). Littleton, CO: Society of Economic Geology. https://doi.org/10.5382/AV100.06

Johnson, A. (2009). MGL0904 cruise, RV Marcus G. Langseth. https://doi.org/10.7284/903749

Karig, D. E. (1970). Ridges and basins of the Tonga-Kermadec island arc system. *Journal of geophysical research*, *75*(2), 239-254. https://doi.org/10.1029/JB075i002p00239

Lallemand, S., Heuret, A., & Boutelier, D. (2005). On the relationships between slab dip, back-arc stress, upper plate absolute motion, and crustal nature in subduction zones. *Geochemistry, Geophysics, Geosystems, 6*(9). https://doi.org/10.1029/2005GC000917

Li, B., Yang, Y., Shi, X., Ye, J., Gao, J., Zhu, A., & Shao, M. (2014). Characteristics of a ridge-transform inside corner intersection and associated mafic-hosted seafloor hydrothermal field (14.0° S, Mid-Atlantic Ridge). *Marine Geophysical Research*, *35*, 55-68. https://doi.org/10.1007/s11001-013-9209-1

Lister, G. S., White, L. T., Hart, S., & Forster, M. A. (2012). Ripping and tearing the rolling-back New Hebrides slab. *Australian Journal of Earth Sciences*, *59*(6), 899-911. https://doi.org/10.1080/08120099.2012.686454

Luyendyk, B. P., Bryan, W. B., & Jezek, P. A. (1974). Shallow structure of the New Hebrides island arc. *Geological Society of America Bulletin*, *85*(8), 1287-1300. https://doi.org/10.1130/0016-7606(1974)85%3C1287:SSOTNH%3E2.0.CO;2

Macfarlane, A., Carney, J.N., Crawford, A.J. and Greene, H.G. (1988). Vanuatu—A review of the onshore geology. In: Greene, H.G., Wong, F.L., (Eds), *Geology and offshore resources of Pacific Island area—Vanuatu region, Circum-Pacific Council for Energy and Mineral Resources Earth Science Series 8*. Houston, Texas: Circum-Pacific Council for Energy and Mineral Resources.

Maillet, P., Ruellan, E., Gérard, M., Person, A., Bellon, H., Cotten, J., ... & Price, R. C. (1995). Tectonics, magmatism, and evolution of the New Hebrides backarc troughs (Southwest Pacific). In Taylor, B. (Ed.), *Backarc basins: Tectonics and magmatism*, (pp. 177-235). New York, NY: Plenum Press.

Martin, A. K. (2013). Double-saloon-door tectonics in the North Fiji Basin. *Earth and Planetary Science Letters*, *374*, 191-203. https://doi.org/10.1016/j.epsl.2013.05.041

Martínez, F., Fryer, P., Baker, N. A., & Yamazaki, T. (1995). Evolution of backarc rifting: Mariana Trough, 20–24 N. *Journal of Geophysical Research: Solid Earth*, *100*(B3), 3807-3827. https://doi.org/10.1029/94JB02466

Meffre, S., & Crawford, A. J. (2001). Collision tectonics in the New Hebrides arc (Vanuatu). *Island Arc*, *10*(1), 33-50. https://doi.org/10.1046/j.1440-1738.2001.00292.x

Molnar, P., & Atwater, T. (1978). Interarc spreading and Cordilleran tectonics as alternates related to the age of subducted oceanic lithosphere. *Earth and Planetary Science Letters*, *41*(3), 330-340. https://doi.org/10.1046/j.1440-1738.2001.00292.x

Monjaret, M. C., Bellon, H., & Maillet, P. (1991). Magmatism of the troughs behind the New Hebrides island arc (RV Jean Charcot SEAPSO 2 cruise): K-Ar geochronology and petrology. *Journal of Volcanology and Geothermal Research*, *46*(3-4), 265-280. https://doi.org/10.1016/0377-0273(91)90088-H

Musgrave, R. J., & Firth, J. V. (1999). Magnitude and timing of New Hebrides Arc rotation: paleomagnetic evidence from Nendo, Solomon Islands. *Journal of Geophysical Research: Solid Earth*, *104*(B2), 2841-2853. https://doi.org/10.1029/1998JB900080

Neely, J. S., & Furlong, K. P. (2018). Evidence of displacement-driven maturation along the San Cristobal Trough transform plate boundary. *Earth and Planetary Science Letters*, *485*, 88-98. https://doi.org/10.1016/j.epsl.2017.12.044

Pelletier, B., (1993). SOPACMAPS.LEG3 cruise, RV L'Atalante. https://doi.org/10.17600/93000252

Pelletier, B., Calmant, S., & Pillet, R. (1998). Current tectonics of the Tonga–New Hebrides region. *Earth and Planetary Science Letters*, *164*(1-2), 263-276. https://doi.org/10.1016/S0012-821X(98)00212-X

Pelletier, B., Lafoy, Y., & Missegue, F. (1993). Morphostructure and magnetic fabric of the northwestern North Fiji Basin. *Geophysical Research Letters*, *20*(12), 1151-1154. https://doi.org/10.1029/93GL01240

Petterson, M. G., Babbs, T., Neal, C. R., Mahoney, J. J., Saunders, A. D., Duncan, R. A., ... & Natogga, D. (1999). Geological–tectonic framework of Solomon Islands, SW Pacific: crustal accretion and growth within an intra-oceanic setting. *Tectonophysics*, *301*(1-2), 35-60. https://doi.org/10.1016/S0040-1951(98)00214-5

Rodriguez, M., Chamot-Rooke, N., Fournier, M., Huchon, P., & Delescluse, M. (2013). Mode of opening of an oceanic pull-apart: The 20° N basin along the Owen fracture zone (NW Indian Ocean). *Tectonics*, *32*(5), 1343-1357. https://doi.org/10.1002/tect.20083

Schellart, W. P., Lister, G. S., & Jessell, M. W. (2002). Analogue modelling of asymmetrical back-arc extension. *Journal of the Virtual Explorer*, *7*, 25-42.

Schellart, W. P., Lister, G. S., & Toy, V. G. (2006). A Late Cretaceous and Cenozoic reconstruction of the Southwest Pacific region: Tectonics controlled by subduction and slab rollback processes. *Earth-Science Reviews*, *76*(3-4), 191-233. https://doi.org/10.1130/0091-7613(2002)030%3C0311:AMOAAB%3E2.0.CO;2

Sdrolias, M., & Müller, R. D. (2006). Controls on back-arc basin formation. *Geochemistry, Geophysics, Geosystems*, *7*(4). https://doi.org/10.1029/2005GC001090

Sleep, N., & Toksöz, M. N. (1971). Evolution of marginal basins. *Nature*, *233*(5321), 548-550. https://doi.org/10.1038/233548a0

Stewart, M. S., Hannington, M. D., Emberley, J., Baxter, A. T., Krätschell, A., Petersen, S., ... & Fassbender, M. L. (2022). A new geological map of the Lau Basin (southwestern Pacific Ocean) reveals crustal growth processes in arc-backarc systems. *Geosphere*, *18*(2), 910-943. https://doi.org/10.1130/GES02340.1

Summer, D. (2024). Mapping outcomes for manuscript titled "Multi-Phase Tectonic and Volcanic Evolution of a Nascent Backarc Rift: Impacts of Spreading Centre Reorientation, Subduction Reversals, Ridge Collisions, and Asymmetric Slab Rollback on the Northern New Hebrides Backarc". Zenodo. https://doi.org/10.5281/zenodo.13844923

Tamaki, K., & Honza, E. (1991). Global tectionics and formation of marginal basins: Role of the western Pacific. *Episodes Journal of International Geoscience*, *14*(3), 224-230. https://doi.org/10.18814/epiiugs/1991/v14i3/005

Taylor, F. W., Bevis, M. G., Schutz, B. E., Kuang, D., Recy, J., Calmant, S., ... & Reichenfeld, C. (1995). Geodetic measurements of convergence at the New Hebrides island arc indicate arc fragmentation caused by an impinging aseismic ridge. *Geology*, *23*(11), 1011-1014. https://doi.org/10.1130/0091-7613(1995)023%3C1011:GMOCAT%3E2.3.CO;2

Taylor, B., & Karner, G. D. (1983). On the evolution of marginal basins. *Reviews of Geophysics*, *21*(8), 1727-1741. https://doi.org/10.1130/0091-7613(1995)023%3C1011:GMOCAT%3E2.3.CO;2

Taylor, B., Zellmer, K., Martinez, F., & Goodliffe, A. (1996). Sea-floor spreading in the Lau back-arc basin. *Earth and Planetary Science Letters*, *144*(1-2), 35-40. https://doi.org/10.1016/0012-821X(96)00148-3

Uyeda, S., & Kanamori, H. (1979). Back-arc opening and the mode of subduction. *Journal of Geophysical Research: Solid Earth*, *84*(B3), 1049-1061. https://doi.org/10.1029/JB084iB03p01049

Wallace, L. M., Ellis, S., & Mann, P. (2009). Collisional model for rapid fore-arc block rotations, arc curvature, and episodic back-arc rifting in subduction settings. *Geochemistry, Geophysics, Geosystems*, *10*(5). https://doi.org/10.1029/2008GC002220

Wright, I. C., Parson, L. M., & Gamble, J. A. (1996). Evolution and interaction of migrating cross-arc volcanism and backarc rifting: An example from the southern Havre Trough (35 20′–37 S). *Journal of Geophysical Research: Solid Earth*, *101*(B10), 22071-22086. https://doi.org/10.1029/96JB01761

Wu, J. E., McClay, K., Whitehouse, P., & Dooley, T. (2009). 4D analogue modelling of transtensional pull-apart basins. *Marine and Petroleum Geology*, *26*(8), 1608-1623. https://doi.org/10.1016/j.marpetgeo.2008.06.007